Circulation Research

ORIGINAL RESEARCH

Ischemic Conditioning Promotes Transneuronal Survival and Stroke Recovery via CD36-Mediated Efferocytosis

Hyunwoo Ju, Il-Doo Kim, Ina Pavlova, Shang Mu, Keun Woo Park, Joseph Minkler, Ahmed Madkoor, Wei Wang, Xiaoman Wang, Zhuhao Wu, Jiwon Yang, Maria Febbraio, John W. Cave, Sunghee Cho

BACKGROUND: Remote ischemic conditioning (RIC) has been implicated in cross-organ protection in cerebrovascular disease, including stroke. However, the lack of a consensus protocol and controversy over the clinical therapeutic outcomes of RIC suggest an inadequate mechanistic understanding of RIC. The current study identifies RIC-induced molecular and cellular events in the blood, which enhance long-term functional recovery in experimental cerebral ischemia.

METHODS: Naive mice or mice subjected to transient ischemic stroke were randomly selected to receive sham conditioning or RIC in the hindlimb at 2 hours post-stroke. At 3 days post-stroke, monocyte composition in the blood was analyzed, and brain tissue was examined for monocyte-derived macrophage (Mφ), levels of efferocytosis, and CD36 expression. Mouse with a specific deletion of CD36 in monocytes/Mφs was used to establish the role of CD36 in RIC-mediated modulation of efferocytosis, transneuronal degeneration, and recovery following stroke.

RESULTS: RIC applied 2 hours after stroke increased the entry of monocytes into the injured brain. In the postischemic brain, Mφ had increased levels of CD36 expression and efferocytosis. These changes in brain Mφ were derived from RIC-induced changes in circulating monocytes. In the blood, RIC increased CD36 expression in circulating monocytes and shifted monocytes to a proinflammatory Lymphocyte antigen 6 complex (LY6C)^{High} state. Conditional deletion of CD36 in Mφ abrogated the RIC-induced monocyte shift in the blood and efferocytosis in the brain. During the recovery phase of stroke, RIC rescued the loss of the volume and of tyrosine hydroxylase+ neurons in substantia nigra and behavioral deficits in wild-type mice but not in mice with a specific deletion of CD36 in monocytes/Mφs.

CONCLUSIONS: RIC induces a shift in monocytes to a proinflammatory state with elevated CD36 levels, and this is associated with CD36-dependent efferocytosis in Mφs that rescues delayed transneuronal degeneration in the postischemic brain and promotes stroke recovery. Together, these findings provide novel insight into our mechanistic understanding of how RIC improves poststroke recovery.

GRAPHIC ABSTRACT: A graphic abstract is available for this article.

Key Words: ischemic stroke ■ macrophages ■ neuroinflammatory diseases ■ neuroprotection ■ phagocygosis

Meet the First Author, see p 454

Stroke is a leading cause of physical disability, but the successful management and treatment of stroke remain to be limited. The difficulties of directly manipulating the brain and accessing agents through BBB are attributed to the limitation. These challenges advocate for the development of alternative strategies, including the use of peripheral systems to influence stroke pathophysiology.

Stroke causes a massive infiltration of peripheral immune cells into the injured brain.[1,2] Two distinct monocyte subsets, representing anti-inflammatory (Lymphocyte antigen 6 complex [Ly6C]^{Low}/CCR2 [C-C

Correspondence to: Sunghee Cho, PhD, Burke Neurological Institute, 785 Mamaroneck Ave, White Plains, NY 10605. Email suc2002@med.cornell.edu
Supplemental Material is available at https://www.ahajournals.org/doi/suppl/10.1161/CIRCRESAHA.124.325428.
For Sources of Funding and Disclosures, see page e49.

Circulation Research is available at www.ahajournals.org/journal/res

Novelty and Significance

What Is Known?

- Infiltrated monocyte–derived macrophages into the postischemic brain cause neural inflammation, but they also engage in efferocytosis that promotes tissue repair in the injured central nervous system.
- Remote ischemic conditioning (RIC) changes monocyte composition and enhances functional recovery in experimental brain ischemia.
- The application of RIC is safe, feasible, and tolerable in patients with stroke, but clinical outcomes remain inconsistent.

What New Information Does This Article Contribute?

- We provide experimental evidence that RIC modifies peripheral monocyte composition and molecular expression and leads to favorable changes in debris clearance, structure integrity, transneuronal degeneration, and behavior following stroke.
- Protective effects of RIC disappear in the absence of CD36 in macrophage, suggesting an essential mechanistic role for CD36 in RIC-induced endogenous protective outcomes.

The current study demonstrates that immune-mediated RIC mechanisms facilitate inflammatory and recovery processes in the injured central nervous system. Given the challenges in directly manipulating the brain after stroke, the study suggests that RIC is a promising alternative strategy by inducing changes in peripheral monocytes that can influence injury progression and recovery. Moreover, RIC-induced peripheral changes uncovered by this study may serve as biomarkers to establish an optimal RIC protocol.

Nonstandard Abbreviations and Acronyms

AC	apoptotic cell
CCR2	C-C motif chemokine receptor 2
cKO$^{MM\varphi}$	mice with a specific deletion of CD36 in monocytes/Mφs
CNS	central nervous system
ContI	contralateral hemisphere
GFP	green fluorescent protein
IpsiI	ipsilateral hemisphere
LDL	low-density lipoprotein
Ly6C	lymphocyte antigen 6 complex
MCAO	middle cerebral artery occlusion
MFI	mean fluorescent intensity
Mφ	macrophage
RIC	remote ischemic conditioning
SNc	substantia nigra pars compacta
TH	tyrosine hydroxylase
TLR	toll-like receptor
WT	wild type

motif chemokine receptor 2]–) and proinflammatory (Ly6C^{High}/CCR2+) monocytes, circulate in mouse blood. Ly6C^{High} monocytes enter the brain during stroke, differentiate into disease-associated macrophages (Mφs; M1φ), and cause neural inflammation. Despite their contribution to tissue damage and infarct development, preventing Ly6C^{High} monocyte entry hinders subsequent stroke recovery.[2–4] This paradoxical role of Mφ derives from their phenotypic conversion from inflammatory M1φ to reparative microglia-like M2φ phenotype in the injury environment.[5–7] This phenotypic plasticity has contributed to the controversy over the function of Mφ and microglia in the injured brain. Identification of the origin and function of Mφ via in situ tracking of peripheral monocytes in the poststroke brain showed the sustained contribution of Mφ to stroke pathology and repair from acute and recovery phases of stroke.[6,7]

In light of the repeated translational failure of neuroprotection-based strategies in stroke, remote ischemic conditioning (RIC), a noninvasive paradigm, has emerged as a potential strategy for clinical application in patients with stroke.[8–11] The conditioning-induced protective mechanisms shared among preischemic, per-ischemic, and postischemic applications have been associated with proinflammatory mediators such as inducible nitric oxide synthase, cytokines, chemokine, TLRs (toll-like receptors), and HMGB1 (high mobility group box 1 protein).[12–17] Several mechanisms, including increased blood flow, changes in neural and circulatory factors, and immune cells, specifically monocytes, have been suggested to mediate cross-organ protection away from the site of ischemic conditioning (eg, limb).[2,18–22] The RIC-induced cross-organ protection from preclinical studies promoted clinical investigation

in stroke. While RIC is safe, feasible, and tolerable in patients with acute ischemic stroke treated with thrombectomy in patients,[23] the effectiveness of the RIC for acute stroke remains uncertain due to the variability of doses and intervals of RIC application.[24–26] Thus, optimization of RIC protocols requires an improved mechanistic understanding of how RIC enhances endogenous protection. Previous studies showed that RIC-induced peripheral monocyte shift to a proinflammatory status promoted stroke recovery in mice, and the absence of the shift in monocyte phenotypes can abolish the RIC-enhanced functional benefit.[2] Still to be delineated are the molecular and cellular events that temporally connect RIC-induced alteration in monocyte composition to behavior outcomes and how acute changes in the blood foster long-term functional improvement.

Mapping longitudinal transcriptome changes in the postischemic brain showed that the most perturbed and persistently upregulated genes in the ipsilateral hemisphere (Ipsil) were related to neuroinflammation and the clearance of cellular debris (efferocytosis).[27] The promotion of efferocytosis is mediated by an orchestrated interaction between danger signals and phagocytic receptors that drive the conversion of disease-associated Mφ to reparative microglia-like Mφ in central nervous system (CNS) environments.[5,28–32] Mechanistically, efferocytosis-induced changes in metabolism, resulting in greater lactate production, promoted the proliferation of reparative Mφ, the key process for tissue resolution.[33,34] In stroke, efferocytosis contributes to hematoma and injury resolution in the postischemic brain.[35–37] CD36, an innate pattern recognition receptor, is expressed in various cell types, including monocytes and Mφ, microvascular endothelial cells, microglia, platelets, and epithelial cells in many tissues.[38,39] CD36 elicits inflammatory innate host responses and clears apoptotic cells (ACs) and debris for tissue resolution.[40–44] Based on this functional duality, we hypothesize that CD36 mediates RIC-associated molecular and cellular changes that promote functional recovery in chronic stroke. Here, we show that monocyte/Mφ-CD36 mediates RIC-induced monocyte shift to a proinflammatory state and efferocytosis, and this shift is associated with an attenuation of transneuronal degeneration and improvement in stroke recovery. These findings suggest that the upregulation of peripheral CD36 is a potential approach to mimic RIC effects.

METHODS

Data Availability

The data of the article can be obtained by sending a reasonable request to the corresponding author.

Detailed methods and the Major Resources Table are provided in the Supplemental Material.

RESULTS

RIC Increases Monocyte Entry and Enhances Mφ Efferocytosis in the Postischemic Brain

We previously showed that RIC applied 2 hours after stroke (postconditioning) induces a shift in monocytes toward a proinflammatory (Ly6C^{High}/CCR2+) subset during the acute phase of stroke, and this shift is necessary for enhanced stroke recovery.[2] This previous study demonstrated that RIC-induced monocyte composition changes in the blood were important for enhanced functional recovery, but the important question of how a monocyte shift in the acute phase resulted in long-term behavior benefit remained unanswered. Because clearing ACs and cellular debris by Mφ is crucial for injury resolution and tissue repair, the present study asked whether RIC-enhanced efferocytosis by monocyte-derived Mφ in the injured brain is a key biological response that connects the temporally distant events of acute cellular change and improved behavior outcome.

To address whether RIC enhanced either the clearance of beads (phagocytosis) or ACs (efferocytosis), mice were subjected to 30-min transient middle cerebral artery occlusion (MCAO) and received either sham conditioning (sham) or RIC at 2 hours after stroke. At 3 days postischemia, brain immune cells were harvested from each hemisphere and analyzed by flow cytometry to assess phagocytosis activity in vivo (Figure 1A). Mφ and microglia were identified as a (CD11b+/CD45+/Lin—) population by excluding (Lin+) T— and B— cells, NK cells, and neutrophils (Figure 1B). Only a (CD45^{Low}) subset was present in the contralateral hemisphere (Contl), whereas the Ipsil contained both (CD45^{High}) and (CD45^{Low}) subsets (Figure 1B).[45] CD45 subset analyses identified (CD45^{Low}) as microglia in the Contl. In the Ipsil, the (CD45^{High}) population is Mφ, and the CD45^{Low} subset is a mixture of microglia and Mφ that have undergone a phenotype change to microglia-like cells.[6] RIC did not increase the number of CD45+ cells in the Contl, but it significantly increased the CD45+ population in the Ipsil. Together, these findings show that RIC promotes the infiltration of circulating monocytes into the injured hemisphere, and these cells adopt a (CD45^{High}) Mφ phenotype (Figure 1C).

To assess in vivo Mφ phagocytosis activity in the brain, fluorescence beads (beads$^{580/605}$) were infused intravenously at 2 days after MCAO (Figure 1A). The beads readily cross the blood-brain barrier and can be phagocytosed by brain immune cells. At 3 days post-stroke, brain cells were dissociated and analyzed by cytometry to count the (CD45+/CD11b+/Lin—) cells containing beads (Figure 1B). Our previous study showed that Mφs, not microglia, are the major phagocytes in the postischemic brain, and circulating monocytes do not phagocytose beads,[6] which indicates that (bead+ CD45+) cells in the postischemic brain in the current study are predominantly Mφs engaging phagocytosis. Flow cytometry

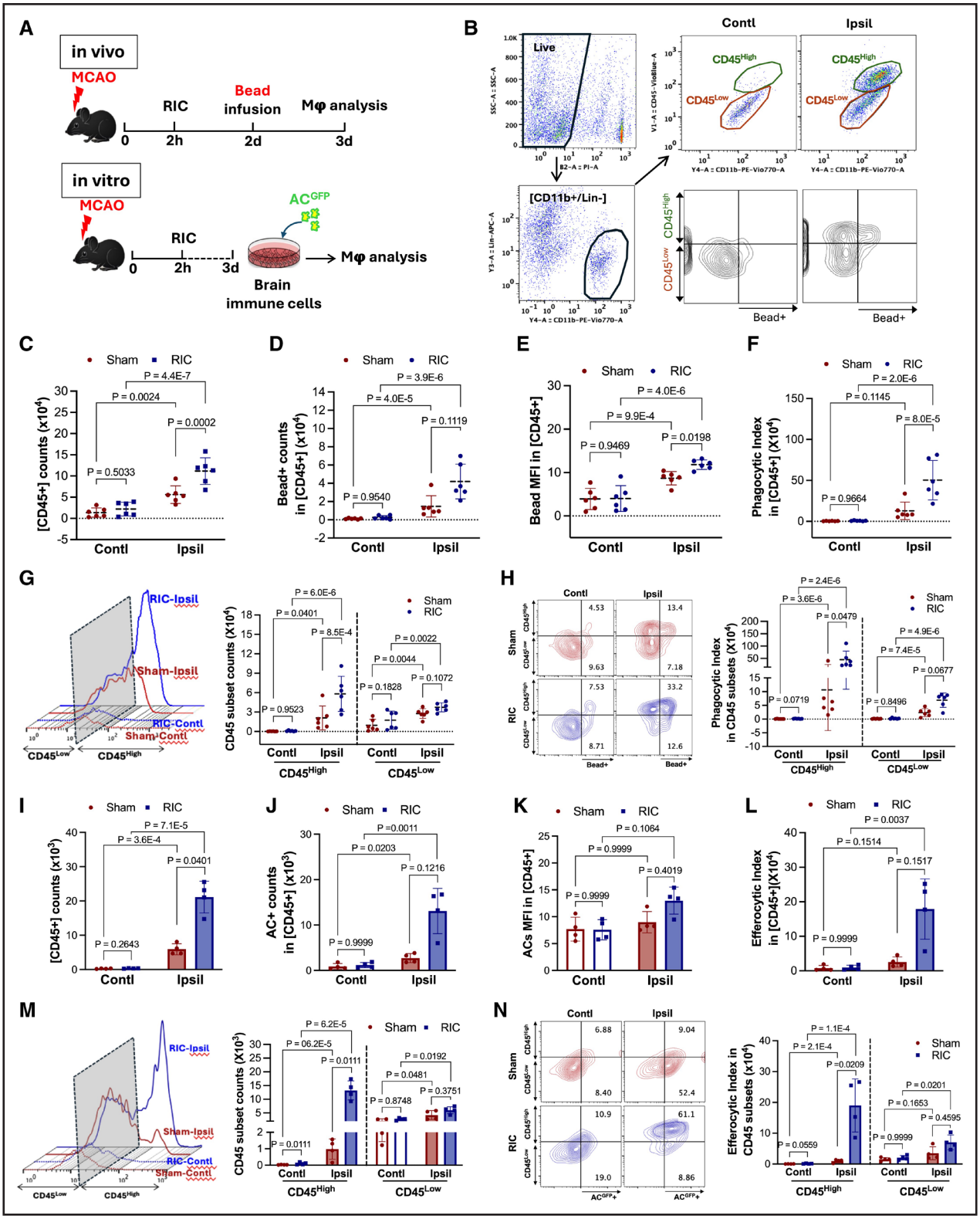

Figure 1. Remote ischemic conditioning (RIC) increases monocyte entry and enhances macrophage (Mφ) phagocytosis in the postischemic brain.

A, Experimental timeline. Mice were subjected to 30-min middle cerebral artery occlusion (MCAO), and RIC was applied 2 h after reperfusion. Immune cells isolated from each hemisphere were analyzed at 3 days post-MCAO. For in vivo phagocytosis assay, beads$^{580/605}$ were infused retro-orbitally into the mice at 2 days post-MCAO. For in vitro efferocytosis assessment, isolated brain immune cells were cultured for 2 hours (2×10^5/well). GFP (green fluorescent protein)-tagged apoptotic cells (AC^{GFP+}) were then added (brain immune cells: AC^{GFP+}=1:5) and cocultured for 1 h. The analysis measured the number of AC^{GFP}+ cells within the (CD45+/CD11b+/Lin−) immune cells. **B**, Gating of (CD45+/CD11b+/Lin−) Mφ/microglia in the postischemic brain to determine bead+ cell number (counts) and mean fluorescent intensity (MFI) of phagocytosis. (*Continued*)

analysis showed that RIC showed an increased trend in the number of beads+ CD45+ cells and significantly increased bead intensity (mean fluorescent intensity [MFI]) in the Ipsil (Figure 1D and 1E). Accordingly, the phagocytosis index (counts×MFI) was significantly and selectively increased in the RIC group (Figure 1F).

Additional flow cytometry analyses addressed whether there were differences in trafficking and phagocytosis levels between the $CD45^{High}$ and $CD45^{Low}$ subsets. RIC significantly increased the number of $CD45^{High}$ cells in Ipsils at 3 days post-stroke (Figure 1G). RIC increased phagocytosis levels in both CD45 subsets at 3 days post-stroke (Figure S2A and S2B), but the magnitude of phagocytosis activity was greater in the $CD45^{High}$ subset (Figure 1H). Given that $CD45^{High}$ Mφs undergo phenotype changes to a microglia-like $CD45^{Low}$ phenotype in the postischemic brain[6,7] and injury environment,[5,28] the increase in the number and phagocytosis levels of $CD45^{Low}$ cells in the current study was likely $CD45^{High}$ Mφs that have adopted the $CD45^{Low}$ reparative phenotype.

To test whether the RIC could also enhance efferocytosis levels in an in vitro model system, we measured the efferocytosis activity of brain immune cells isolated 3 days post-MCAO, which were cocultured with ACs (Figure 1A). To generate ACs, isolated cultured splenocytes were placed under UV light for 30 min.[46] Splenocytes cultures were also labeled with GFP (green fluorescent protein) using GFP-Cell Linker (>99% GFP labeling efficiency and ≈70% were ACs; Figure S3). After 1 hour of coculture with ACs, brain immune cells (CD45+/CD11b+/Lin—) isolated from the Ipsil of stroked mice treated with RIC contained a higher number of cells that contained significantly higher AC^{GFP+} cells compared with either brain immune cells isolated from the Contl or from sham-treated mice (Figure 1J and 1L). This confirmed the in vivo findings that RIC enhances immune cells in the Ipsil from mice, leading to elevated levels of efferocytosis and MFI.

Additional analyses of the cultured brain immune cells also showed that cells isolated from stroked mice treated with RIC contained a significantly higher number of $CD45^{High}$ cells in the Ipsil (Figure 1M). Moreover, RIC significantly enhanced efferocytosis activities in $CD45^{High}$subsets (Figure 1N), and the enhancement is mainly from the increased number of AC^{GFP+} Mφs and not from an increased efferocytosis capacity (MFI; Figure S4A and S4B). Taken together, the in vivo and in vitro findings show that RIC enhances monocyte trafficking into the injured hemisphere and increases the Mφ population and phagocytosis/efferocytosis activity in the postischemic brain. These effects collectively indicate that RIC can modulate the peripheral immune system to CNS injury and the subsequent repair processes.

RIC-Induced CD36 Expression Enhances Phagocytosis in the Postischemic Brain

Longitudinal mapping of transcriptome changes in the mouse brain for 6 months after stroke showed that the most perturbed and persistently upregulated genes are related to neuroinflammation and pattern recognition of clearance of cellular debris and ACs (National Center for Biotechnology Information Short Read Archive; accession number: PRJNA525413)[27] (Figure S5A and S5B). CD36 is a class B scavenger receptor involved in innate host immunity and efferocytosis[40–44,47] that has elevated expression for months after stroke (Figure S5B), suggesting that CD36 may be an effector molecule for RIC-induced immune modulation in Mφs.

To establish whether CD36 mediates, at least in part, the effects of RIC on the peripheral immune system following stroke and the subsequent repair processes, we initially addressed whether RIC impacted CD36 expression levels in (CD45+/CD11b/Lin—) cells in the postischemic brain at 3 days (Figure 2A). Stroke increased the number of CD36+ cells (Figure 2B) and CD36 expression levels (MFI; Figure 2C) for both sham and RIC groups in the Ipsil. Compared with the sham group, the increases were significantly larger in the RIC group (Figure 2B and 2C). The RIC-induced increase in CD36+ cells occurred in both CD45 subsets although the increase in the $CD45^{High}$ subset was significantly higher (3.1-fold versus 1.5-fold increase for $CD45^{High}$ and $CD45^{Low}$, respectively; Figure 2E). RIC increased CD36 expression (MFI) only in the $CD45^{High}$ subset (Figure 2F).

Because CD36 expression in Mφ positively correlates with phagocytosis activity,[37] we tested whether RIC modulated CD36-mediated phagocytosis. Mice were infused with $beads^{580/605}$ at 2 days post-stroke, and then, the (CD45+/CD11b+/Lin—) cells in the brain were isolated and analyzed at 3 days post-ischemia (Figure 1A). For CD36-/CD45+ cells, RIC did not impact either the

Figure 1 Continued. **C** through **H**, In vivo analyses (n=6/group). Effect of RIC on the number of phagocytes and phagocytosis in (CD45+/CD11b+/Lin—) populations. CD45+ Mφ/microglia count (**C**), bead+ cell count (**D**), MFI of bead+ cells (**E**), phagocytic index (bead+ counts×bead MFI) (**F**), CD45+ Mφ/microglia counts in CD45 subsets (**G**), and phagocytosis index in CD45 subsets (**H**). **I** through **N**, In vitro analyses (n=4/group) of RIC effects on the number of phagocytes and efferocytosis in (CD45+/CD11b+/Lin—) populations. CD45+ Mφs/microglia count (**I**), AC+ cell count (**J**), MFI of AC+ cells (**K**), efferocytosis index (AC+ counts×AC MFI; **L**), CD45+ Mφ/microglia counts in CD45 subsets (**M**), and efferocytosis index in CD45 subsets (**N**). Statistical significance was assessed with 2-way ANOVA followed by the post hoc Fisher Least Significant Difference test (**C** and **E**–**G**) and the Scheirer-Ray-Hare test followed by the Conover-Iman test for post hoc analyses (**D**, **H**, and **I**–**L**). **C** through **N**, Analyses were performed using the average value of triplicate measurements per animal. Contralateral hemisphere (Contl) vs ipsilateral hemisphere (Ipsil) (effect of stroke); sham conditioning (sham) vs RIC (effect of RIC).

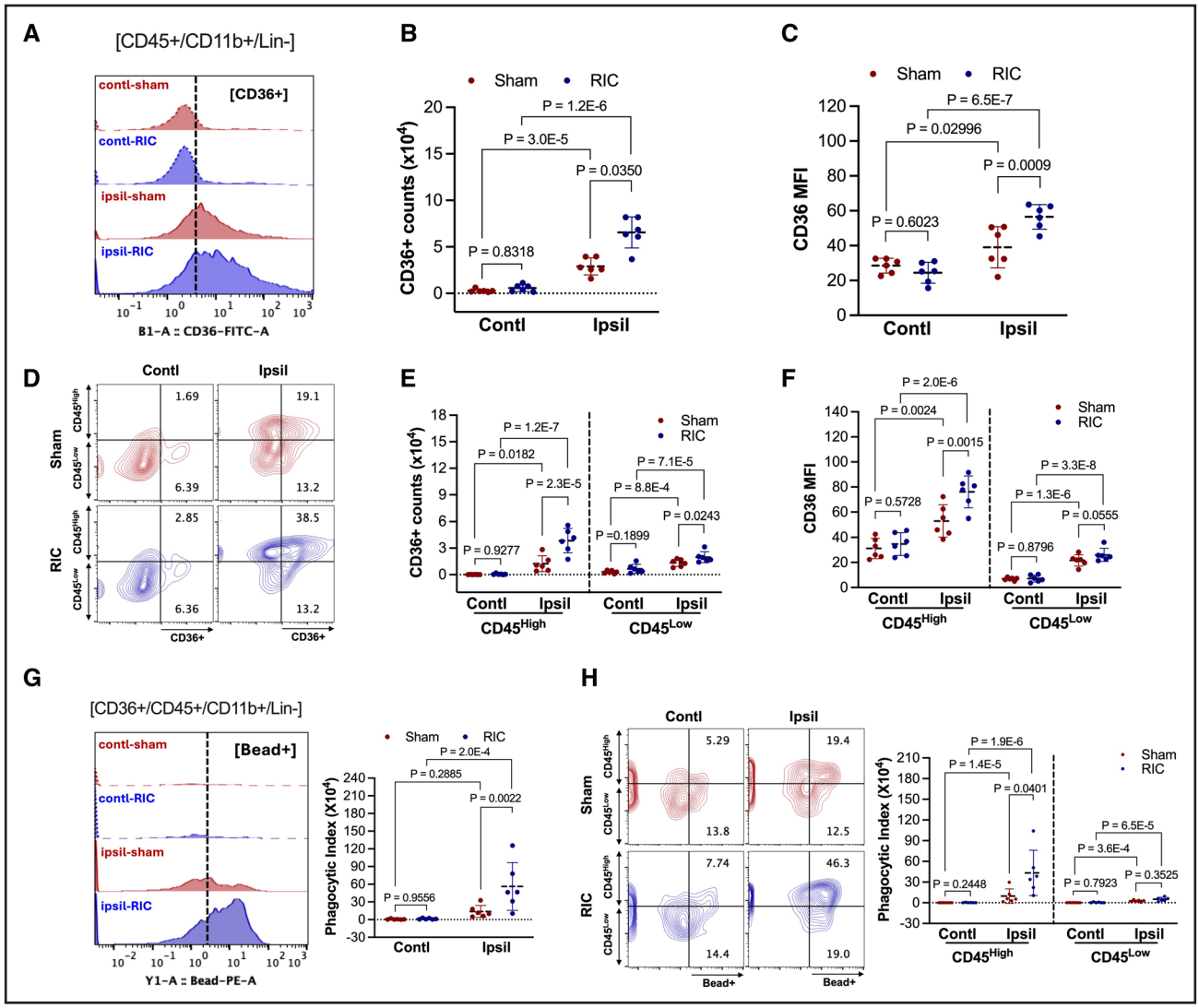

Figure 2. Remote ischemic conditioning (RIC)–induced CD36 expression enhances phagocytosis in the postischemic brain. Brain immune cells were isolated at 3 days post-stroke from the contralateral hemisphere (Contl) and ipsilateral hemisphere (Ipsil) of sham conditioning (sham) or RIC animals. **A** through **C**, Analyses of CD36 expression in (CD45+/CD11b+/Lin−) cells. CD36 flow histogram in sham and RIC animals (**A**), number of CD36+ cells (**B**), and CD36 expression (by mean fluorescent intensity [MFI]) in total CD45+ cells. **D** through **F**, Analyses of CD36 expression in $CD45^{High}$ and $CD45^{Low}$ subsets in (CD45+/CD11b+/Lin−) populations. Flow diagram (**D**), number of CD36+ cells (**E**), and CD36 expression (**F**) in CD45 subsets. **G** and **H**, Phagocytosis assay in CD36+ cells in (CD45+/CD11b+/Lin−) cells (**G**) and CD45 subsets (**H**). n=6/group. **B** through **H**, Analyses utilized the mean of triplicate measurements for each animal. Statistical significance was assessed using 2-way ANOVA with the Fisher Least Significant Difference test (**C**–**G**) and the Scheirer-Ray-Hare test with the Conover-Iman post hoc analysis (**B** and **H**). Contl vs Ipsil (effect of stroke); sham vs RIC (effect of RIC).

number of bead+ cells, the bead MFI, or phagocytosis activity when compared between either Contl versus Ipsil (Figure S6A through S6C) or between $CD45^{High}$ and $CD45^{Low}$ subsets (Figure S6D through S6F). By contrast, RIC significantly increased bead+ and bead MFI (Figure S7A and S7B), as well as phagocytosis (Figure 2G), for CD36+ cells within the Ipsil, compared with the Contl and compared with the sham. RIC significantly increased bead+ cells and bead MFI in both $CD45^{High}$ and $CD45^{Low}$ subsets in the Ipsil (Figure S7C and S7D), which resulted in significantly higher phagocytosis levels, especially for the $CD45^{High}$ subset (Figure 2H). Together, these results show that RIC augments stroke-induced CD36 expression and CD36-mediated phagocytosis in the injured brain. Moreover, the higher levels of CD36+/$CD45^{High}$ cells in the Ipsil of RIC-treated mice after stroke suggest that peripherally derived CD36+ Mφ has a major role in the RIC-enhanced phagocytosis in the postischemic brain.

CD36 Mediates an RIC-Induced Monocyte Shift to a Proinflammatory State

Because previous work showed that the periphery is the major source of CD36-expressing cells in the postischemic brain,[48] we next addressed whether RIC triggers upregulation of CD36 expression in circulating

monocytes before they enter the injured brain. To determine the effect of RIC on CD36 expression in monocytes, RIC was applied to naive mice without stroke to avoid stroke-induced monocyte mobilization to the injured brain. The blood from naive wild-type (WT) mice with either RIC or sham was collected at 1 day post-RIC, and CD36 expression in monocytes was analyzed by flow cytometry (Figure 3A, bottom left). RIC did not alter the number of either total or CD36+ monocytes (Figure 3B and 3C), but it did significantly increase CD36 expression levels in monocytes (Figure 3D). Circulating monocytes in mice are a heterogeneous population of proinflammatory Ly6C^{High} (CCR2+) and anti-inflammatory Ly6C^{Low} (CCR2—) subsets. In consistent with the previous report of RIC-induced monocyte shifts to a proinflammatory state (increased Ly6C$^{High/Low}$ ratio),[2] the analysis of peripheral monocytes in naive mice in this current study showed that RIC increased Ly6C^{High} monocytes without altering an Ly6C^{Low} subset (Figure 3E, left) and generated an overall shift toward a proinflammatory state (Figure 3E, right). Moreover, RIC-enhanced CD36 expression occurred selectively in Ly6C^{High} monocytes (Figure 3F), which is the subset that enters the postischemic brain. The RIC-induced upregulation of CD36 in Ly6C^{High} monocytes, thus, accounts for the increases in the number of CD36+ monocytes (Figure 2B and 2E) and the CD36 MFI (Figure 2C and 2F) in the postischemic brain. Compared with CD45^{High} Mφ in the brain after stroke, however, the RIC-mediated increase in CD36 levels in circulating Ly6C^{High} monocytes was proportionately less (Figure 2F versus Figure 3F). These findings indicate that RIC triggers an increase in CD36 expression within peripheral monocytes and suggest that the abundance of CD36 ligands in the injured brain[49–52] further elevates CD36 expression levels following their infiltration into the Ipsil.

To establish the necessity of CD36 for the RIC-induced monocyte shift, we analyzed monocytes in mice with a constitutive CD36 deletion (CD36KO). This analysis found that RIC neither induced a change in the number of monocytes nor a shift in subsets (Figure 3G). The interpretation of these findings is confounded, however, by the fact that CD36 is expressed in many cell types and tissues. To assess the role of CD36 specifically in monocyte/Mφ, mice with a specific deletion of CD36 in monocytes/Mφs (cKO^{MMφ}) were analyzed (Figure S8). Like the CD36KO mice, an RIC-induced change in either the number of monocytes or shift monocyte subsets was absent in cKO^{MMφ} mice (Figure 3H). The disappearance of the subset shifts in both CD36KO and cKO^{MMφ} mice demonstrates that CD36 expression in monocytes/Mφ is necessary for the RIC-induced shift in monocyte inflammatory states.

The requirement for CD36 expression in monocytes/Mφ was also tested in vitro by incubating splenocytes with sera from RIC or sham mice (Figure 3I). Compared with cultures treated with sera from sham mice, WT splenocytes treated with sera from RIC-treated mice showed a significant increase in the Ly6C^{High} subset and a decrease in the Ly6C^{Low} subset, which increased Ly6C$^{High/Low}$ ratio (Figure 3J). By contrast, cKO^{MMφ} splenocytes treated with sera from RIC-treated mice did not induce shifts in monocyte subsets (Figure 3K). Together with the in vivo findings, these findings show that CD36 is required for RIC-induced changes in both monocyte composition and the shift in monocyte inflammatory state.

cKO^{MMφ} Mice Delay Stroke Recovery

The monocyte shift to an inflammatory state is required for promoting recovery in a chronic phase of stroke,[2] and this shift is abrogated in cKO^{MMφ} mice. We next examined whether the loss of CD36 in Mφ impacted stroke outcomes. Compared with the WT genotype, cKO^{MMφ} mice had similar mortality during an acute phase of stroke, comparable stroke-induced body weight loss, and similar infarct size when assessed at 3 days post-ischemia (Figure 4A and 4C). The number of cells in the CD45^{High} subset within the Ipsil was also similar, suggesting that monocyte trafficking between the WT and cKO^{MMφ} genotypes was comparable (Figure 4D). The number of the CD45^{Low} cells, however, was significantly larger in both the Ipsil and Contl of cKO^{MMφ} mice (Figure 4D), suggesting that the loss of CD36 in Mφ/monocytes influences the microglia populations and Mφ that adopt a microglia-like CD45^{Low} phenotype.

Early motor deficits and recovery of ambulatory function in mouse stroke models are, to a certain degree, clinical representations of impairment and recovery in patients with stroke. To model clinical features of motor function, we used open field tests to assess overall locomotion.[53] Despite similar acute outcomes, cKO^{MMφ} mice displayed greater motor deficits than the WT mice. Longitudinal open field tests showed that cKO^{MMφ} mice underperformed in traveling distance and less time in the center in an open field compared with their pre-stroke baselines (Figure 4E). We measured hindlimb grip strength as an assessment of stroke-induced catabolic events that result in muscle mass loss.[54] The cKO^{MMφ} mice also reduced grip strength of the hind limbs compared with WT mice (Figure 4F). The rotarod test is a striatal-based motor learning and locomotion assessment tool that gauges motor function impairment following a stroke.[53] The analyses, however, showed no difference in rotarod performance between genotypes (Figure 4G). Unlike open field and grip strength tests, which showed similar prestroke baseline between genotypes, rotarod showed a significant difference in baseline between the genotypes (232.1±29.4 versus 187.4±45.4 s for WT and cKO^{MMφ}; WT: n=9; cKO^{MMφ}: n=10/genotype; P=0.0223). This suggests that cKO^{MMφ} mice had impaired motor learning ability during pretraining, and this may mask

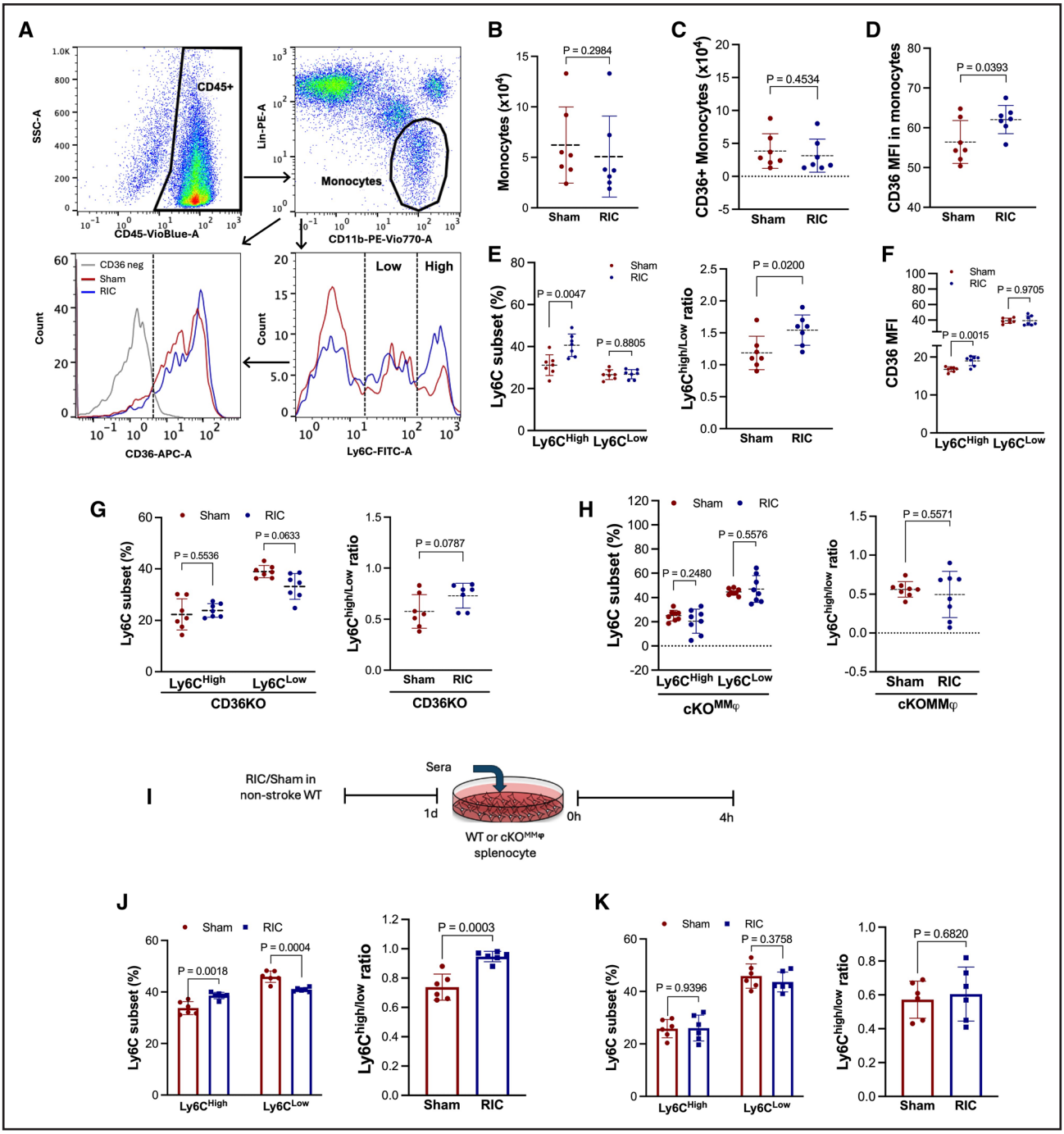

Figure 3. CD36 mediates a remote ischemic conditioning (RIC)–induced monocyte shift to a proinflammatory state.
The blood of naive nonstroke mice was analyzed 1 day after sham conditioning (sham) or RIC. n=7/group **A**, Flow gating strategy in the blood of naive nonstroke mice 1 day after sham or RIC. Histogram shows CD36 expression in monocytes (lower left) and monocyte Lymphocyte antigen 6 complex (Ly6C) subsets (lower right); n=7/group. **B** through **D**, Quantification of total number of circulating monocytes (CD45+/CD11b+/Lin−), CD36+ monocytes, and CD36 expression (mean fluorescent intensity [MFI]) in monocytes. **E**, Effect of RIC on monocyte subsets, percentage of Ly6C^{High} and Ly6C^{Low} monocyte subsets (left) and Ly6C$^{High/Low}$ ratio (right; **F**), and CD36 MFI in the Ly6C monocyte subsets. **G** and **H**, Effect of RIC on Ly6C^{High} or Ly6C^{Low} monocyte subsets (left) and Ly6C$^{High/Low}$ ratio (right) in CD36KO mice (**G**; n=7) and mice with a specific deletion of CD36 in monocytes/Mφs (cKO^{MMφ}; **H**; n=8). **I**, Sera were harvested 1 day after sham or RIC in naive wild-type (WT) mice. Splenocytes were incubated with sham or RIC-sera for 4 hours, and monocyte subsets were analyzed. **J** and **K**, Percentage of Ly6C^{High} or Ly6C^{Low} monocyte subsets (**left**) and the Ly6C $^{High/Low}$ ratio (**right**) in WT splenocytes (**J**; n=3/group) and cKO^{MMφ} splenocytes (**K**; n=3/group). **B** through **K**, Analyses were conducted using the average of triplicate measurements per animal. Statistical significance was assessed with the Student *t* test (**D**–**K**) or the Mann-Whitney *U* test (**B** and **C**) in sham vs RIC.

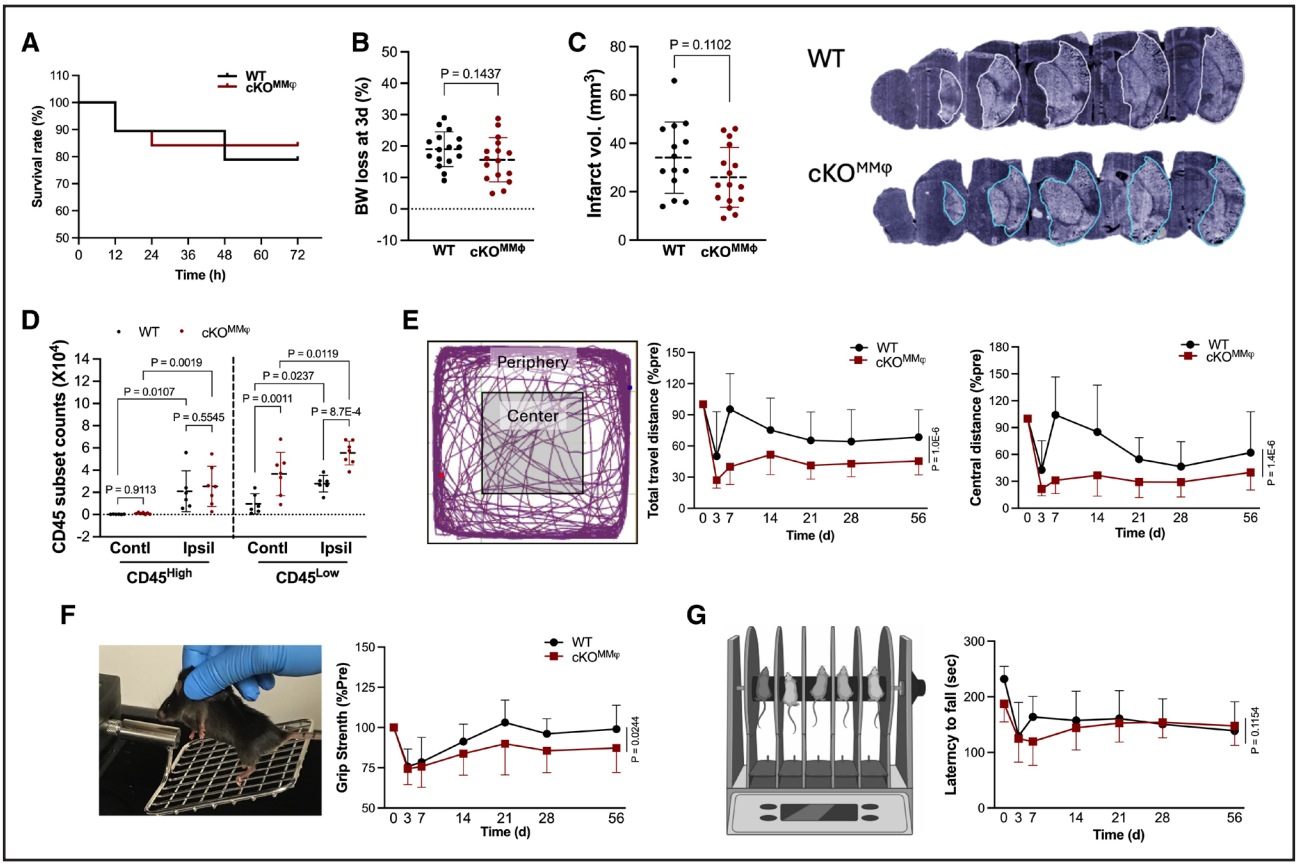

Figure 4. Mice with a specific deletion of CD36 in monocytes/Mφs (cKO^{MMφ}) delay stroke recovery.
A, Assessment of survival rate in wild-type (WT; CD36$^{fl/fl}$) and cKO^{MMφ} during an acute phase of stroke (WT: n=19; cKO^{MMφ}: n=20 at a starting point). **B**, Assessment of body weight loss (% prestrike baseline) at 3 days post-middle cerebral artery occlusion (MCAO); n=16 **C**, Indirect (edema corrected) infarct volume at 3 days post-MCAO (WT: n=14; cKO^{MMφ}: n=16). Representative infarct images at 3 days post-MCAO in WT and cKO^{MMφ} mice. **D**, Flow analyses of CD45 subset in (CD11b+/Lin−) populations (WT: n=6; cKO^{MMφ}: n=7). Analyses were performed using the average value of triplicate measurements per animal. **E** through **G**, Longitudinal poststroke behavior test in WT or cKO^{MMφ} mice (WT: n=7; cKO^{MMφ}: n=9). Open field test to assess total travel distance and distance in the center zone against prebaseline (% pre, **E**), grip strength against prebaseline (% pre, **F**), and rotarod (**G**). For assessing statistical significance, a Student *t* test was conducted to evaluate the effect of genotypes (**B** and **C**), and a 2-way ANOVA followed by the post hoc Fisher Least Significant Difference test was used to analyze the effects of stroke or genotype (**D**–**G**). Contl indicates contralateral hemisphere; and Ipsil, ipsilateral hemisphere.

differences in recovery from stroke-induced motor deficits. The overall delayed stroke recovery in cKO^{MMφ} mice reveals the importance of CD36-expressing Mφ for functional recovery in stroke.

Stroke-Induced Efferocytosis Is Reduced in cKO^{MMφ} Mice

To address that CD36 was necessary for RIC-enhanced efferocytosis, we determined the effect of Mφ-CD36 deletion on efferocytosis in the postischemic brain. WT and cKO^{MMφ} brain immune cells isolated at 3 days post-ischemia were incubated with GFP-labeled ACs (AC^{GFP+}; Figure 1A, in vitro). Because the monocyte infiltration, indicated by the CD45^{High} subset, was comparable between WT and cKO^{MMφ} mice (Figure 4D), the same number of brain immune cells (2×10^5/well) from these mice were cultured for efferocytosis assay. For WT cells, stroke increased the number of AC^{GFP+} cells and their MFI (Figure 5B and 5C), leading to significantly enhanced efferocytosis activities (Figure 5D). For cKO^{MMφ} cells, despite stroke-induced increases in the number of AC^{GFP+} cells and MFI (Figure 5B and 5C), the efferocytosis index in cKO^{MMφ} did not reach significance and was significantly lower compared with WT cells (Figure 5D). These findings show that stroke selectively enhances efferocytosis in the Ipsil of WT but not in cKO^{MMφ} mice.

Additional analyses of the CD45 subsets within cKO^{MMφ} brain immune cells showed reduced efferocytosis in both subsets but a greater relative reduction in the CD45^{High} subset (Figure 5H). The reduction in the CD45^{High} subset derived from a reduction in the number of AC^{GFP+} cells and MFI (Figure 5F and 5G), whereas the reduction in the CD45^{Low} subset resulted from reduced MFI (Figure 5G). Taken together, these findings show that CD36 expression in Mφ is required for stroke-induced efferocytosis in the Ipsil.

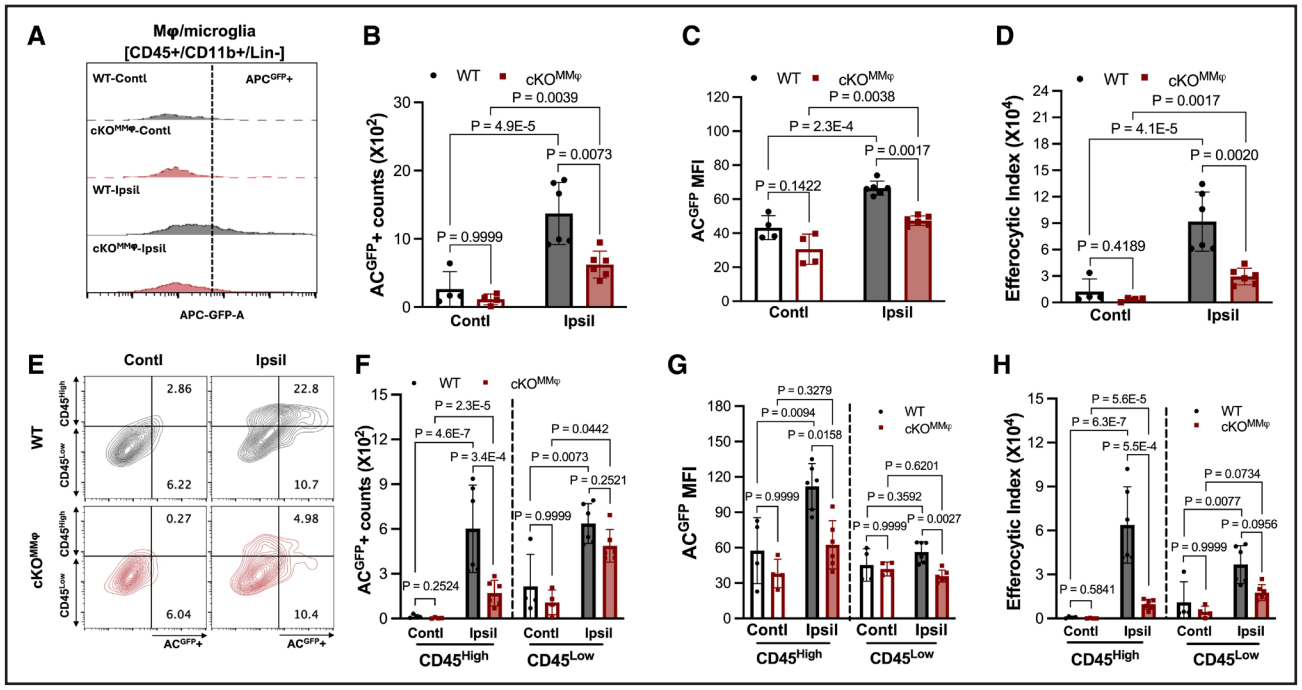

Figure 5. Stroke-induced efferocytosis is reduced in the mice with a specific deletion of CD36 in monocytes/Mφs (cKO^{MMφ}). Green fluorescent protein-tagged apoptotic cells (AC^{GFP+}) were added to the cultures (brain cells: ACs, 1:5) for 1 h and analyzed AC^{GFP}+ cells in (CD45+/CD11b+/Lin−) macrophages (Mφs)/microglia. **A**, Flow histogram of AC^{GFP}+ cells in Mφs/microglia. **B** through **D**, Quantification of AC^{GFP+}-Mφs/microglia count (**B**), AC^{GFP+}-Mφs/microglia mean fluorescent intensity (MFI; **C**), and efferocytosis index (AC^{GFP+} counts×AC^{GFP+} MFI; **D**). **E**, Flow contour plot of AC^{GFP}+ CD45^{High} and CD45^{Low} Mφs/microglia. **F** through **H**, Quantification of AC^{GFP+} counts in CD45 subsets (**F**), AC^{GFP+} MFI in CD45 subsets (**G**), and efferocytosis index (AC^{GFP+} counts×AC^{GFP+} MFI) in CD45 subsets (**H**). Wild type (WT)-contralateral hemisphere (Contl): n=4; WT-ipsilateral hemisphere (Ipsil): n=6; cKO^{MMφ}-Contl: n=4; cKO^{MMφ}-Ipsil: n=6. Analyses utilized the mean of triplicate measurements for each sample animal. Statistical significance was assessed using the Scheirer-Ray-Hare test with the Conover-Iman post hoc analysis. Contl vs Ipsil (effect of stroke); WT vs cKO^{MMφ} (effect of genotype).

CD36 Mediates RIC-Enhanced Phagocytosis in the Postischemic Brain

The required monocyte shift for RIC-promoted stroke recovery[2] and the contribution of CD36 expression in Mφ for the monocyte phenotype shift and phagocytosis together suggest that Mφ-CD36 mediates RIC-enhanced efferocytosis in the postischemic brain. Thus, we used cKO^{MMφ} mice to address whether CD36 was required for RIC-enhanced phagocytosis. Unlike RIC-enhanced efferocytosis in WT (C57) mice (Figure 1C and 1F), applying RIC to cKO^{MMφ} mice did not increase either the number of Mφ/microglia (Figure 6A) or phagocytosis activity (bead+ count, MFI, and phagocytosis index; Figure 6B and 6D). Analysis of CD45 subset showed that RIC significantly increased phagocytosis in CD45^{High} (and CD45^{Low}) subsets in WT mice (Figure 1H), but RIC with cKO^{MMφ} mice had no effect on the number of CD45^{High} and CD45^{Low} cells (Figure 6E), phagocytic cells, MFI (Figure S9A and S9B), or phagocytosis activities (Figure 6F) in both CD45 subsets. Similar findings were seen with cultured brain immune cells from cKO^{MMφ} mice, where RIC had no effect on the number of Mφ/microglia (Figure 6G) and efferocytosis activities (Figure 6H and 6J). Moreover, RIC did not influence the number of Mφ/microglia (Figure 6K) and efferocytosis activities in CD45 subsets (Figure S9C and S9D; Figure 6L). Given that the CD45^{High} subset represents infiltrating monocyte-derived Mφ into the injured brain, the absence of the RIC effects in cKO^{MMφ} mice reveals the importance of Mφ-CD36 in mediating RIC-enhanced efferocytosis in the injured CNS.

RIC Attenuates Dopaminergic Neuron Loss in Substantia Nigra in Chronic Stroke

MCAO-induced striatal and cortical infarction causes progressive atrophy in the primary infarcted tissue and remote areas.[55–59] The progressive brain atrophy is accompanied by sustained immune activation and continuous infiltration of peripheral immune cells into primary and delayed entry to secondary injury sites in the brain.[7,27] In the substantia nigra pars compacta (SNc), M-Mφ was absent during the acute phase (3 days post-stroke) but became abundant and engaged in phagocytosis (engulfing beads) during the chronic phase (2 months post-stroke), showing the contribution of M-Mφ to SNc transneuronal degeneration. Therefore, we investigated the effect of RIC on the progression of brain atrophy by analyzing volume in the brain subregions at 2 months post-ischemia. The ischemic stroke in sham-conditioned animals showed brain atrophy throughout the Ipsil and primary injury sites, including the

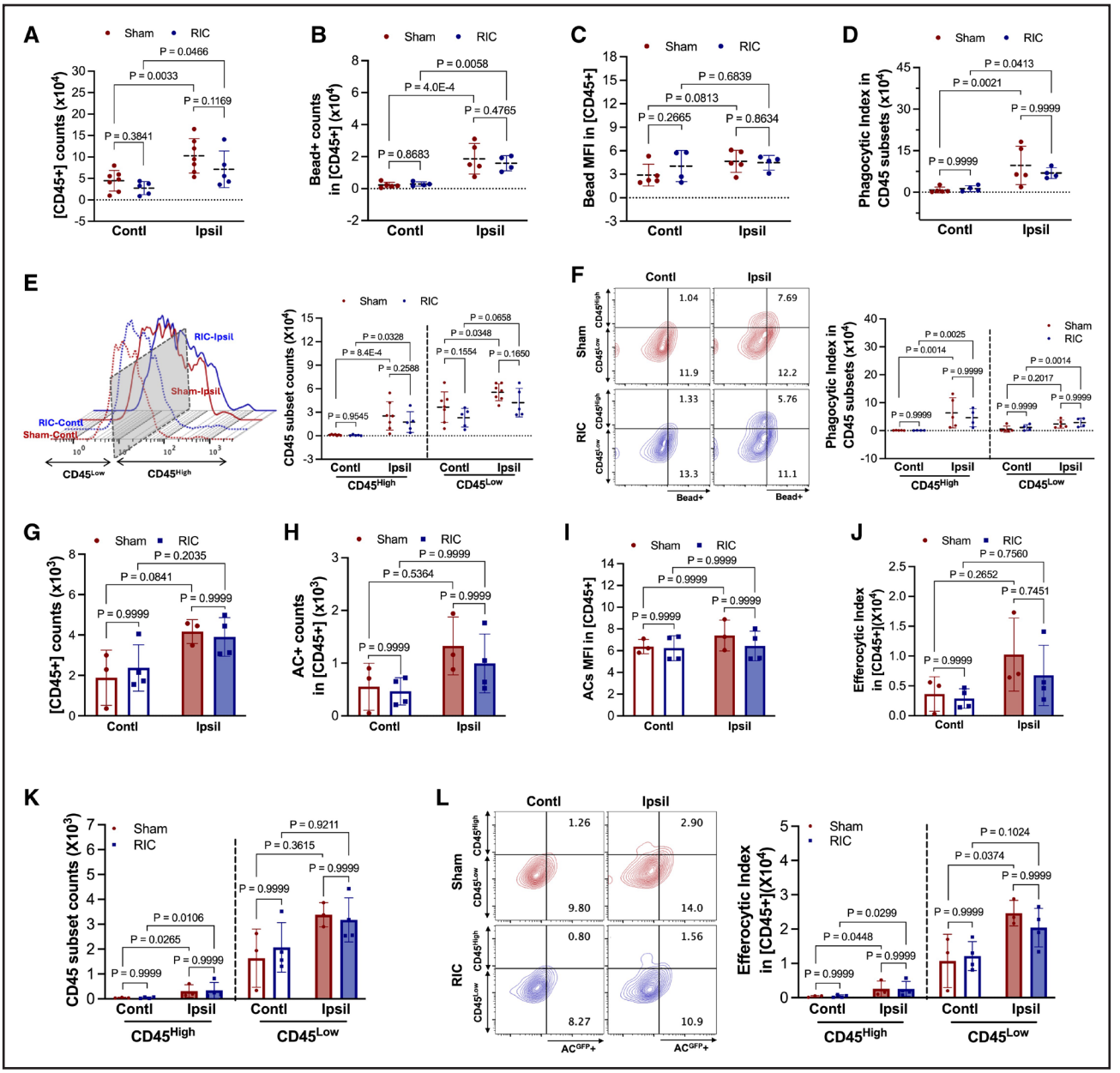

Figure 6. CD36 mediates remote ischemic conditioning (RIC)–enhanced phagocytosis in the postischemic brain.
Mice with a specific deletion of CD36 in monocytes/Mφs (cKO^{MMφ}) with 30-min middle cerebral artery occlusion (MCAO) were subjected to sham conditioning (sham) or RIC at 2 hours post-MCAO. Beads$^{580/605}$ were infused retro-orbitally at 2 days post-MCAO, and immune cells isolated from each hemisphere were analyzed at 3 days. **A**, Total (CD45+/CD11b+/Lin−) macrophage (Mφ)/microglia counts in cKO^{MMφ} mice (sham: n=7; RIC: n=5). **B** through **D**, In vivo phagocytosis assay (sham: n=5; RIC: n=4). The number of beads$^{580/605}$+ cells in cKO^{MMφ} Mφ/microglia (**B**), beads$^{580/605}$+ mean fluorescent intensity (MFI; **C**), and phagocytic index (beads$^{580/605}$+ counts×beads$^{580/605}$+ MFI; **D**). **E**, Representative histogram for total (CD45+/CD11b+/Lin−) Mφ/microglia number in CD45 subsets (sham: n=7; RIC: n=5). **F**, Flow contour plot of cKO^{MMφ} mice for the number of beads$^{580/605}$+ cells in CD45^{High} and CD45^{Low} Mφ/microglia. Sham: n=5; RIC: n=4. **G** through **L**, in vitro analyses (n=4/group) of RIC effects on the number of phagocytes and efferocytosis assay in cKO^{MMφ} mice. **G**, (CD45+/CD11b+/Lin−) Mφs/microglia count. **H**, AC+ Mφs/microglia count. **I**, MFI of AC+ cells. **J**, Efferocytosis index (AC+ counts×AC+ MFI). **K**, CD45^{High} and CD45^{Low} Mφs/microglia count. **L**, Flow contour plot of cKO^{MMφ} mice for AC+ cells and efferocytosis index in CD45^{High} and CD45^{Low} Mφs/microglia. Analyses were conducted using the average of triplicate measurements for each animal (**A**–**L**). Statistical significance was assessed with the Scheirer-Ray-Hare test followed by the Conover-Iman test for post hoc analyses. Contralateral hemisphere (Contl) vs ipsilateral hemisphere (Ipsil; effect of stroke); sham vs RIC (effect of RIC).

striatum and cortex (Figure S10A through S10C), as well as the thalamus, which receives input from the striatum and projects to the cortex (Figure S10D). Stroke-induced brain atrophy was also associated with ventricular hypertrophy (Figure S10G). Other remote areas, however, such as the hypothalamus and hippocampus, were not impacted (Figure S10E and S10F).[60] Despite a previous study showing RIC enhances stroke recovery,[2] our subregion and ventricle volume assessment showed that RIC did not significantly prevent atrophy in the primary

and secondary injury sites and ventricular enlargement (although the ratios of ipsilateral/contralateral ventricles showed a trend toward reduction of hypertrophy in the RIC group; Figure S10G). This analysis, however, used tissue at 2 months to estimate the brain and ventricle volume. Interanimal variability in the glia scar formation surrounding the injured areas could have masked the effect of RIC, and this led us to investigate the impact of RIC in transneuronal degeneration.

The striatum receives dopaminergic input from TH (tyrosine hydroxylase)-expressing neurons in the SNc. Transneuronal degeneration in SNc is only evident during chronic phases of stroke and not in the acute phase.[7,55,56] To probe the effect of RIC on the neuronal loss in the SNc, we used transgenic mice that express GFP in TH+ neurons ($Tg^{TH\text{-}GFP+}$). Three-dimensional whole-brain imaging shows GFP expression in the olfactory bulb, SNc, and locus coeruleus, and the horizontal view shows GFP expression of TH+ fibers in the striatum (Figure 7A). Immunostaining with TH antibody confirmed that the GFP-expressing cells are TH+ neurons (Video S1). We used Imaris software to analyze the SNc volume and the number of TH+ cells in the SNc in both hemispheres (Figure 7B). Stroke reduced SNc volume in the ipsilateral brain in both sham and RIC mice, but the reduction was significantly attenuated in RIC mice (Figure 7C). Stroke also reduced the number of TH+ neurons in the SNc in sham animals, but there was no significant reduction in RIC animals. The stroke-induced TH+ neuron loss between sham and RIC groups, however, did not reach statistical significance (Figure 7D). Collectively, these findings highlight the effect of RIC in preserving SNc volume and TH+ neurons against stroke-induced degeneration.

To address whether RIC-rescued SNc volume and TH+ neurons are the result of reduced striatal infarction in RIC animals, we compared animals based on the severity of striatal atrophy. At 2 months post-stroke, striatal atrophy varied within both sham and RIC groups, but the mean striatal atrophy was comparable between the groups (Figure S11). Pairwise comparison between sham and RIC groups in animals with small, moderate, or large atrophy showed that RIC mice displayed larger SNc volumes (Figure 7E) and higher TH+ neuronal cell counts (Figure 7F) in the ipsilateral substantia nigra compared with sham animals with similar atrophy. The striatal atrophy-independent rescue of SNc structure suggests that RIC limits transneuronal degeneration independent of stroke-induced primary infarction.

Mφ-CD36 Deletion Abrogates RIC-Attenuated Transneuronal Degeneration and Enhances Stroke Recovery

To investigate the role of CD36 in RIC-induced structure and function relationship, TH+ neuron loss in SNc and functional recovery were assessed in WT and $cKO^{MM\phi}$ mice. Compared with sham mice, RIC significantly increased the number of surviving TH+ neurons in the Ipsil at 2 months post-stroke (Figure 8A). The attenuation of the TH+ cell loss is associated with improved motor function in the open field, increased grip strength, and rotarod performance in chronic stroke (Figure 8C and 8F). In $cKO^{MM\phi}$, RIC did not attenuate TH+ neuron loss (Figure 8B).

The absence of protection from secondary degeneration is associated with no improvement in motor function (Figure 8G, 8H, and 8J) and grip strength, which was significantly worse in RIC mice (Figure 8I). The structural and functional studies, thus, showed that CD36 mediates RIC-attenuated transneuronal degeneration in SNc and stroke recovery. These results collectively showed the importance of CD36 in the RIC effect by upregulation of CD36 expression in circulating monocytes, increasing their entry into the injured brain, enhanced efferocytosis during an acute phase of stroke, mitigating transneuronal degeneration, and promoting functional recovery in chronic stroke (Figure 8K).

DISCUSSION

This study demonstrates that CD36-mediated efferocytosis in monocyte-derived Mφ is a critical mechanistic component of RIC that mediates the attenuation of transneuronal degeneration and promotes stroke recovery. Neural inflammation followed by the resolution of inflammation is the cardinal feature of stroke pathophysiology. These processes are dependent on the infiltration of peripheral immune cells, primarily monocytes, into the injured brain. These pivotal roles played by monocytes advocate for the development of strategies to target these cells to influence injury progression and tissue repair. RIC is a promising noninvasive and clinically viable approach for cross-organ protection,[9,10] but the application of RIC in patients with stroke has been controversial. The current study, however, provides novel insight into the molecular and cellular events underlying the acute changes in the blood following RIC that facilitates long-term functional recovery in experimental cerebral ischemia. A key finding in this study is that RIC-enhanced CD36 expression in monocytes and CD36-mediated efferocytosis in Mφs is required to attenuate delayed transneuronal degeneration in the postischemic brain and promote stroke recovery. Together, these findings suggest that RIC is an effective strategy to manipulate monocytes in the peripheral immune system, which influences injury progression and tissue repair following stroke.

The Mechanism by Which RIC Increases CD36 Expression in the Periphery

An important event triggered by RIC is an increase in CD36 expression within circulating monocytes that do

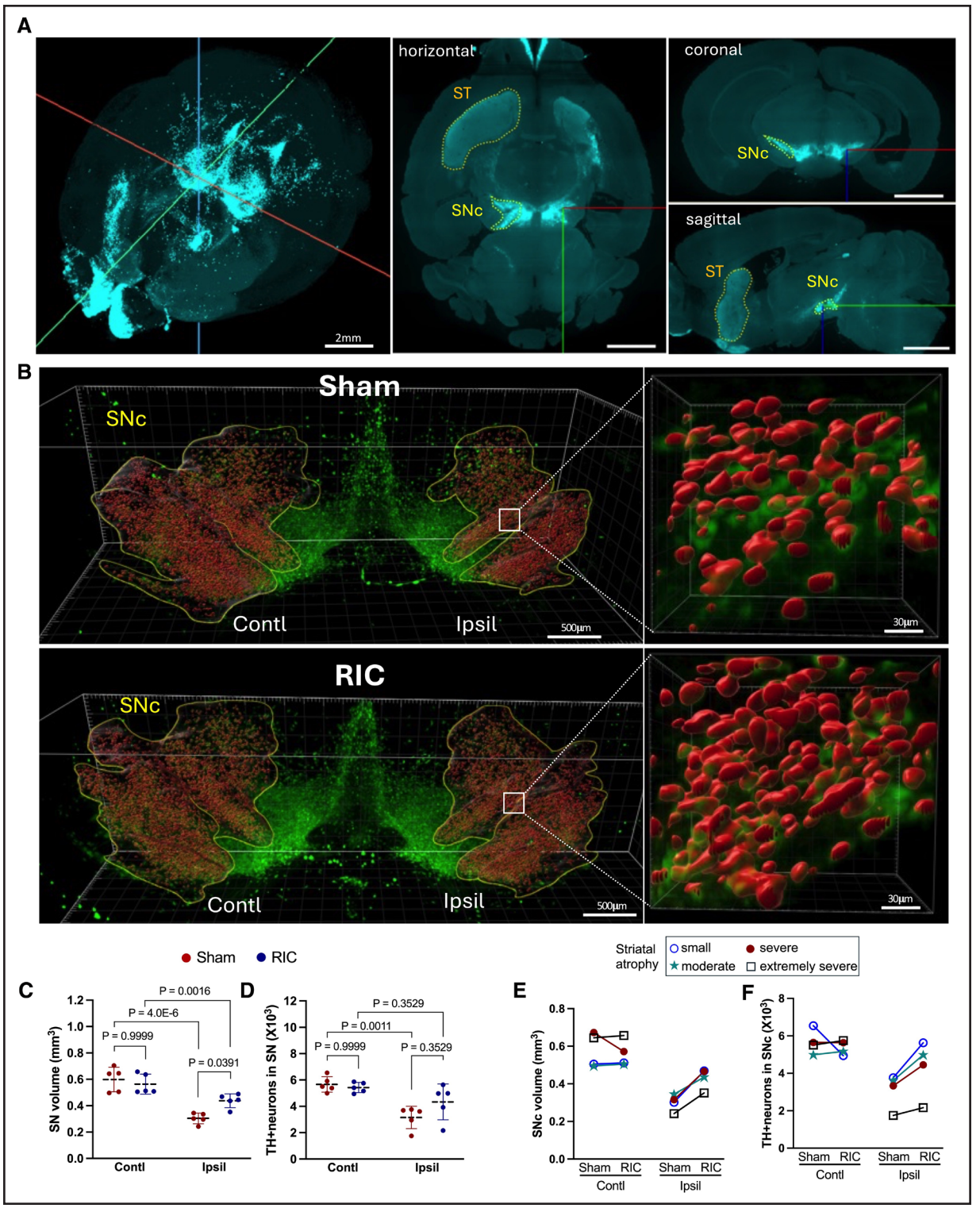

Figure 7. Remote ischemic conditioning (RIC) attenuates dopaminergic neuron loss in substantia nigra pars compacta (SNc) in chronic stroke.

Mice expressed GFP (green fluorescent protein) in TH (tyrosine hydroxylase) neurons ($Tg^{TH\text{-}GFP+}$) were subjected to 30-min middle cerebral artery occlusion (MCAO), and sham conditioning (sham) or RIC was applied 2 h after reperfusion. Brain images were obtained at 2 months postischemia. n=5/group. **A**, Three-dimensional whole-brain image with horizontal, coronal, and sagittal views. GFP+ expression in TH+ cells. Scale bar, 2 mm. **B**, Three-dimensional images of SNc indicated by yellow boundaries, and the red represents areas where TH+ neurons are present. High resolution of SNc showing individual TH+ neurons in the ipsilateral hemisphere. Scale bars, 500 μm for whole-SNc images and 30 μm for magnified images. All representative images were selected to represent the group average across all available data. **C** and **D**, Quantification of SNc volume (indicated by yellow outline) and TH+ neurons indicated by red in yellow boundaries. **E** and **F**, Pairwise analysis of SNc volume (**C**) and TH+ neuron number (**D**) based on the severity of striatal atrophy. The Scheirer-Ray-Hare test followed by the Conover-Iman test for post hoc analyses. Contralateral hemisphere (Contl) vs ipsilateral hemisphere (ipsil; effect of stroke); sham conditioning (sham) vs RIC (effect of RIC). ST indicates striatum.

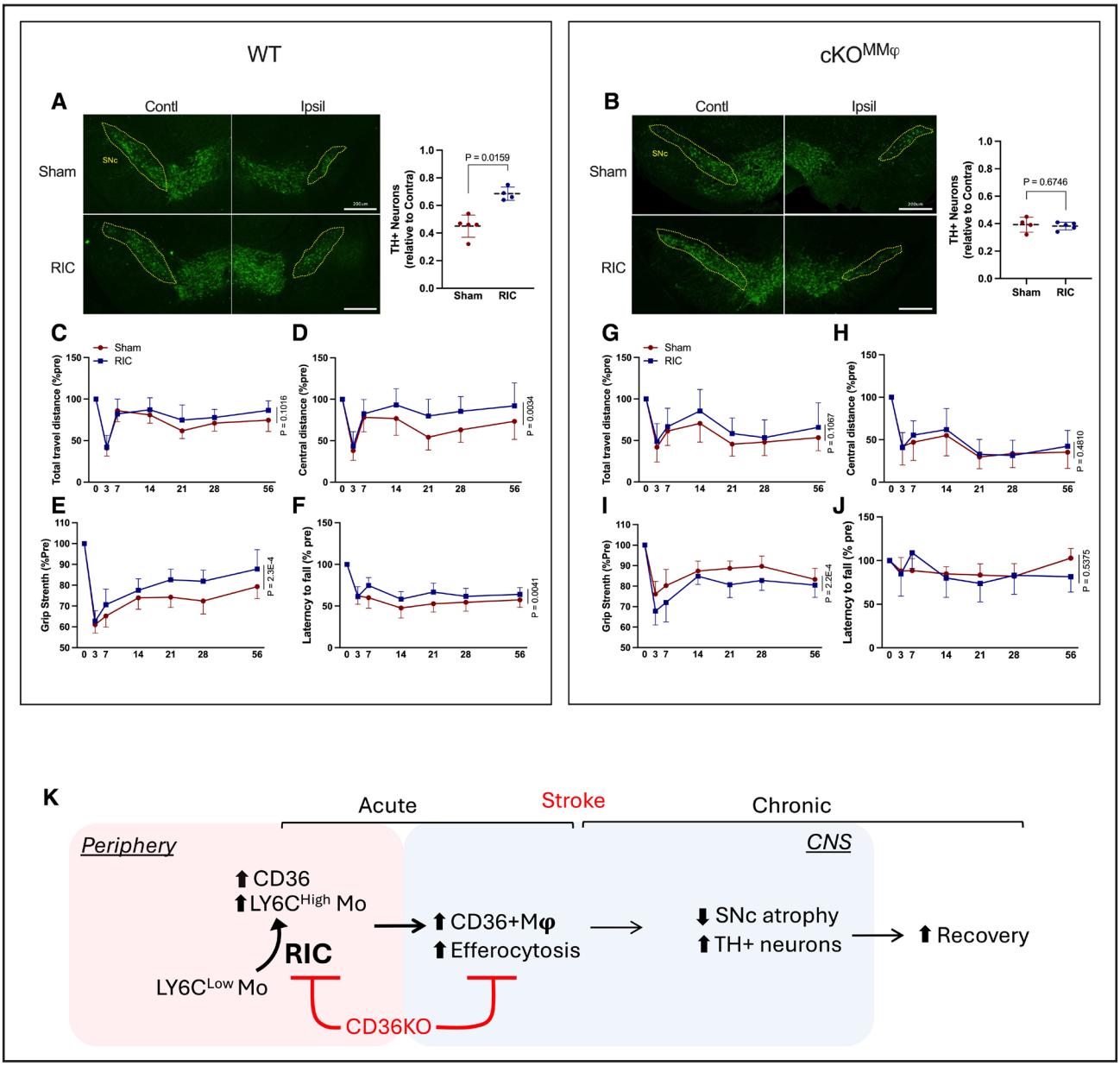

Figure 8. Macrophage (Mφ)-CD36 deletion abrogates remote ischemic conditioning (RIC)–attenuated transneuronal degeneration and enhances stroke recovery.
Wild-type (WT; CD36$^{fl/fl}$) and mice with a specific deletion of CD36 in monocytes/Mφs (cKO^{MMφ}) mice with middle cerebral artery occlusion (MCAO) were received sham conditioning (sham) or RIC at 2 h after MCAO. **A** and **B**, TH (tyrosine hydroxylase) immunofluorescence staining in the brain sections at 2 months after MCAO in WT (**A**) and cKO^{MMφ} (**B**) mice. WT-sham: n=5; WT-RIC: n=4; cKO^{MMφ}-sham: n=4; and cKO^{MMφ}-RIC: n=5. Scale bar, 200 μm. All representative images were selected to represent the group average across all available data. The average values obtained from the 2 sections (−2.8 and −3.4 from bregma) were used for each animal. The number of TH+ cells was measured in both hemispheres and expressed as ratios of ipsilateral/contralateral. The Mann-Whitney *U* test was conducted in sham vs RIC. **C** through **F**, Longitudinal poststroke behavior test in WT mice (sham: n=28; RIC: n=19). **G** through **J**, Longitudinal poststroke behavior test cKO^{MMφ} mice; n=14/group. **C**, **D**, **G**, and **H**, Open field test to assess total travel distance and distance in the center zone. Grip strength in the hind limbs (**E** and **I**) and rotarod (**F** and **J**). Data were presented as percent of prestroke baseline (% pre). Two-way ANOVA followed by the post hoc Fisher Least Significant Difference test was used to analyze the effects of stroke or RIC. **K**, Diagram depicting RIC-induced biological responses in stroke.

not alter the total number of CD36+ monocytes (Figure 3C and 3D). A likely mechanism for the increase in CD36 expression within monocytes is the availability of CD36 ligands in circulation. Repeated episodes of ischemia-reperfusion with RIC produce oxidative stress and a sudden release of reactive oxygen/nitrogen species from mitochondria.[61–63] Activation of CD36 by the presence of abundant ligands (eg, oxidized or modified LDL [low-density lipoprotein] Ox/m) generated by RIC drives a feed-forward upregulation of CD36 expression.[64,65] An important finding in this study is that the increase in CD36 expression is specific to Ly6C^{High} monocytes. The

absence of CD36 upregulation in Ly6C^{Low} monocytes could be due to the higher CD36 baseline in this subset (Figure 3F), which may reflect the patrolling nature of this subset along the endothelium for interacting damaged and ACs, and modified forms of LDL in the vasculature.[66] Ly6C^{High} monocytes, however, are the primary monocyte that infiltrates the injured brain via the CCR2-MCP1 (monocyte chemoattractant protein-1) axis, and their migration underlies the elevated levels of CD36+/CD45^{High} Mφ in the postischemic brain (Figure 2E and 2F).

CD36-Mediated Efferocytosis in the Injured CNS

The function of CD36 in eliciting and suppressing inflammation is context-dependent.[37,67,68] Given that CD36 functions in clearing cellular debris for tissue repair, the RIC-driven enhancement of CD45^{High} Mφ with greater efferocytosis activity is the cellular mechanisms that underlie the protective effect of RIC in the postischemic brain. While the engulfment of synthetic beads in the brain may not represent in vivo efferocytosis, images of Iba1+ phagocytes colocalizing with neurons and neutrophils in the postischemic brain (Figure S12) suggest that efferocytosis occurs in the injured brain. The RIC-mediated increase in Iba1+ cell efferocytosis of neurons and neutrophils in WT mice, but not in cKO^{MMφ} mice (Figure S12), further suggests that RIC-enhanced efferocytosis occurs in a CD36-dependent manner.

An important question, however, is how the enhanced efferocytosis in infarcted tissue during acute stroke preserves TH+ neurons at 2 months post-stroke and promotes long-term stroke recovery in a CD36-dependent manner. Efferocytosis is a crucial step in resolving tissue injury that converts inflammatory Mφs to a reparative phenotype[6] that is proliferating and proresolving.[33] In situ tracking of labeled monocytes in mice with stroke showed that monocyte-derived Mφs are the predominant phagocytes that also have significantly greater efferocytosis capacity than microglia in the ischemic brain.[6] The ability of RIC to promote the resolution of inflammation in stroke is supported by studies that have reported a reduction both in perihematomal edema in patients with hemorrhagic stroke[69] and brain swelling in mice with ischemic stroke.[2] Mechanistically, this resolution requires CD36, as evidenced by lowered efferocytosis levels when CD36 is deleted in Mφs, but the lack of CD36 does not completely abolish efferocytosis (Figure 5) and indicates that there are additional receptors that engage efferocytosis. Moreover, several factors also influence efferocytosis levels, including the nature of phagocytes (professional versus nonprofessional), and the ratio between phagocytic and ACs.[70,71] In addition, efferocytosis can occur in either single or multiple, continuous rounds, the latter of which may be CD36-dependent. Continual efferocytosis is mechanistically distinct from a single round of efferocytosis and relies heavily on the metabolism of ingested AC cargo.[46] Disruption of continual efferocytosis delays injury resolution and expands the necrotic core in atherosclerosis.[72] Transporting long-chain fatty acids via CD36 to the cells provides fuels for fatty acid oxidation, which sustains the activation of reparative Mφs,[68] and may facilitate RIC-enhanced continual efferocytosis and tissue resolution.

CD36 in RIC-Rescued Structure and Function

Proximal MCA occlusion produces an infarct that is primarily in the striatum but also part of the cortex. The long-term injury, however, is not restricted to the primary injury sites because damage spreads into remote areas in a delayed manner, such as the thalamus and SNc.[7] In this study, the structure-function analyses demonstrated that RIC preserves SNc neurons and enhances stroke recovery in a CD36-dependent manner. The faster, CD36-dependent resolution in the acute phase of stroke likely accounts for the protection of the secondary structure and functional benefit in RIC animals. Notably, RIC rescue of SNc volume and TH+ neurons in the Ipsil was not dependent on the severity of striatal atrophies (except for 1 animal with extremely severe striatal atrophy; Figure 7E and 7F). Similarly, RIC-enhanced motor recovery in mice with severe stroke was also comparable to those with smaller infarction.[2] Therefore, the CD36-dependent, but infarct size-independent, benefits of RIC indicate that a timely and rapid resolution, rather than infarct severity, in the primary injury sites determines subsequent structure integrity and behavior. This also suggests that CD36 is a key target for accelerating injury resolution with RIC-induced structural and functional benefits.

Peripheral Markers to Predict RIC Benefit

Stroke with brain atrophy is associated with less favorable recovery,[73] and retrospective imaging studies in patients with ischemic stroke have shown that secondary degeneration in the substantia nigra is associated with poor stroke outcomes.[74,75] The findings in this study show that RIC can attenuate secondary degeneration and promote recovery, which suggests that RIC can be a clinical strategy to preserve brain structural integrity in remote areas and improve stroke recovery. The outcome of RIC clinical trials on patients with acute stroke has been controversial,[24–26] likely due to several issues, including inconsistency including age, comorbidities, stroke subtypes, the time of RIC initiation, and compliance.[76–80] By defining important mechanistic events underlying RIC, as we have done in this study, this will facilitate the establishment of mechanism-based protocols for RIC dosage, frequency, and intervals in repeated RIC applications. Using RIC to target peripheral changes in CD36+ monocytes, this

non-CNS-directed immune strategy may also enable the optimization of RIC protocols to use minimal dosing at maximal intervals to improve compliance issues.

Limitations

Previous studies have demonstrated that phenotypic plasticity of phagocytes in the injured tissue environment and efferocytosis can drive peripheral-derived CD45^{High} Mφs to adopt a microglia-like CD45^{Low} phenotype.[6,7] These phenotype changes in monocyte-derived Mφs prevented assessing the contribution of CD45^{Low} Mφ to efferocytosis because the CD45^{Low} subset also contains resident microglia. Because efferocytosis can promote the proliferation of proresolving Mφs,[33] we suspect that the increased bead+ cells in the CD45^{Low} subset (Figure 1H) are likely due to the proliferation of efferocytosing Mφs that have changed to a reparative Mφ phenotype. The study also has some limitations in statistical analyses. Applying multiple comparisons using the Fisher Least Significant Difference tests following 2-way ANOVA may lower statistical power. An additional caveat is the impact of comorbidities on RIC benefits. Recent studies indicate that obesity impedes the RIC-mediated increase in CD36 expression and monocyte shift, and the disruption of these peripheral changes prevents improvements in recovery from stroke.[80] Further studies are required to assess how RIC interacts with other comorbidities, including diabetes, dyslipidemia, and aging, to optimize RIC-based interventions and improve stroke recovery.

ARTICLE INFORMATION

Received September 03, 2024; revision received January 10, 2025; accepted January 14, 2025.

Affiliations

Burke Neurological Institute, White Plains, NY (H.J., I.P., K.W.P., J.M., A.M., S.C.). Department of Anatomy, Inha University School of Medicine, Incheon, South Korea (I.-D.K.). Helen & Robert Appel Alzheimer's Disease Research Institute (S.M., W.W., X.W., Z.W.) and Feil Brain Mind Research Institute (H.J., S.M., K.W.P., W.W., X.W., Z.W., S.C.), Weill Cornell Medicine, New York, NY. Department of Dentistry and Dental Hygiene, University of Alberta, Edmonton, Canada (M.F.). InVitro Cell Research, Englewood, NJ (J.W.C.). Innovation & Product Development, The Jackson Laboratory, Sacramento, CA (J.Y.).

Acknowledgments

The authors gratefully acknowledge the Burke Neurological Institute Structural and Functional Imaging Core (grants NIHS10OD028547, NIHS10OD036432, and NYS DoH C38326GG to Edmund Hollis) for their support and assistance in this work.

Author Contributions

H. Ju performed efferocytosis assay and flow cytometry analyses in vivo or in vitro studies and wrote the article. I.-D. Kim performed stroke modeling. I. Pavlova performed immunofluorescence studies, and cell counts and volumetric measurements in 3-dimensional images. S. Mu processed the 3-dimensional volumetric data. K.W. Park performed immunofluorescence studies. J. Minkler performed the neurological assessment. A. Madkoor preformed the brain atrophy measurement. W. Wang performed whole-brain clearing, labeling, and imaging. X. Wang generated the 3-dimensional visualization. Z. Wu designed the whole mount test together with collaborators. J. Yang generated mice with a specific deletion of CD36 in monocytes/Mφs line and established protocols for remote ischemic conditioning and flow analyses. M. Febbraio generated CD36$^{fl/fl}$ mice and wrote the article. J.W. Cave provided transgenic tyrosine hydroxylase-GFP positive (Tg$^{TH\text{-}GFP+}$) mice and wrote the article. S. Cho designed the overall study, analyzed data, and wrote the article. I.-D. Kim and J. Yang executed this study at the Burke Neurological Institute.

Sources of Funding

This work was supported by the National Institutes of Health grants NS111568 and NS103326 (to S. Cho).

Disclosures

None.

Supplemental Material

Figures S1–S12
Video S1
References 81–88

REFERENCES

1. Auffray C, Sieweke MH, Geissmann F. Blood monocytes: development, heterogeneity, and relationship with dendritic cells. *Annu Rev Immunol*. 2009;27:669–692. doi: 10.1146/annurev.immunol.021908.132557
2. Yang J, Balkaya M, Beltran C, Heo JH, Cho S. Remote postischemic conditioning promotes stroke recovery by shifting circulating monocytes to CCR2+ proinflammatory subset. *J Neurosci*. 2019;39:7778–7789. doi: 10.1523/JNEUROSCI.2699-18.2019
3. Pedragosa J, Miro-Mur F, Otxoa-de-Amezaga A, Justicia C, Ruiz-Jaen F, Ponsaerts P, Pasparakis M, Planas AM. CCR2 deficiency in monocytes impairs angiogenesis and functional recovery after ischemic stroke in mice. *J Cereb Blood Flow Metab*. 2020;40:S98–S116. doi: 10.1177/0271678X20909055
4. Wattananit S, Tornero D, Graubardt N, Memanishvili T, Monni E, Tatarishvili J, Miskinyte G, Ge R, Ahlenius H, Lindvall O, et al. Monocyte-derived macrophages contribute to spontaneous long-term functional recovery after stroke in mice. *J Neurosci*. 2016;36:4182–4195. doi: 10.1523/JNEUROSCI.4317-15.2016
5. Chen HR, Sun YY, Chen CW, Kuo YM, Kuan IS, Tiger Li ZR, Short-Miller JC, Smucker MR, Kuan CY. Fate mapping via CCR2-CreER mice reveals monocyte-to-microglia transition in development and neonatal stroke. *Sci Adv*. 2020;6:eabb2119. doi: 10.1126/sciadv.abb2119
6. Ju H, Park KW, Kim ID, Cave JW, Cho S. Phagocytosis converts infiltrated monocytes to microglia-like phenotype in experimental brain ischemia. *J Neuroinflammation*. 2022;19:190. doi: 10.1186/s12974-022-02552-5
7. Park KW, Ju H, Kim ID, Cave JW, Guo Y, Wang W, Wu Z, Cho S. Delayed infiltration of peripheral monocyte contributes to phagocytosis and trans-neuronal degeneration in chronic stroke. *Stroke*. 2022;53:2377–2388. doi: 10.1161/STROKEAHA.122.038701
8. Dirnagl U, Becker K, Meisel A. Preconditioning and tolerance against cerebral ischaemia: from experimental strategies to clinical use. *Lancet Neurol*. 2009;8:398–412. doi: 10.1016/S1474-4422(09)70054-7
9. Hoda MN, Bhatia K, Hafez SS, Johnson MH, Siddiqui S, Ergul A, Zaidi SK, Fagan SC, Hess DC. Remote ischemic perconditioning is effective after embolic stroke in ovariectomized female mice. *Transl Stroke Res*. 2014;5:484–490. doi: 10.1007/s12975-013-0318-6
10. Zhou Y, Fathali N, Lekic T, Ostrowski RP, Chen C, Martin RD, Tang J, Zhang JH. Remote limb ischemic postconditioning protects against neonatal hypoxic-ischemic brain injury in rat pups by the opioid receptor/Akt pathway. *Stroke*. 2011;42:439–444. doi: 10.1161/STROKEAHA.110.592162
11. McDonald MW, Dykes A, Jeffers MS, Carter A, Nevins R, Ripley A, Silasi G, Corbett D. Remote ischemic conditioning and stroke recovery. *Neurorehabil Neural Repair*. 2021;35:545–549. doi: 10.1177/15459683211011224
12. Izuishi K, Tsung A, Jeyabalan G, Critchlow ND, Li J, Tracey KJ, Demarco RA, Lotze MT, Fink MP, Geller DA, et al. Cutting edge: high-mobility group box 1 preconditioning protects against liver ischemia-reperfusion injury. *J Immunol*. 2006;176:7154–7158. doi: 10.4049/jimmunol.176.12.7154
13. Gao X, Zhang H, Takahashi T, Hsieh J, Liao J, Steinberg GK, Zhao H. The Akt signaling pathway contributes to postconditioning's protection against stroke; the protection is associated with the MAPK and PKC pathways. *J Neurochem*. 2008;105:943–955. doi: 10.1111/j.1471-4159.2008.05218.x
14. Zhu Y, Ohlemiller KK, McMahan BK, Park TS, Gidday JM. Constitutive nitric oxide synthase activity is required to trigger ischemic tolerance in mouse retina. *Exp Eye Res*. 2006;82:153–163. doi: 10.1016/j.exer.2005.06.005

15. Wang Y, Reis C, Applegate R 2nd, Stier G, Martin R, Zhang JH. Ischemic conditioning-induced endogenous brain protection: applications pre-, per- or post-stroke. *Exp Neurol*. 2015;272:26–40. doi: 10.1016/j.expneurol.2015.04.009
16. Gesuete R, Stevens SL, Stenzel-Poore MP. Role of circulating immune cells in stroke and preconditioning-induced protection. *Acta Neurochir Suppl*. 2016;121:39–44. doi: 10.1007/978-3-319-18497-5_7
17. Cho S, P E-M, Zhou P, Frys K, Ross ME, Iadecola C. Obligatory role of inducible nitric oxide synthase in ischemic preconditioning. *J Cerebral Blood Flow and Metab*. 2005;25:493–501. doi: 10.1038/sj.jcbfm.9600058
18. Kono Y, Fukuda S, Hanatani A, Nakanishi K, Otsuka K, Taguchi H, Shimada K. Remote ischemic conditioning improves coronary microcirculation in healthy subjects and patients with heart failure. *Drug Des Devel Ther*. 2014;8:1175–1181. doi: 10.2147/DDDT.S68715
19. Hoda MN, Siddiqui S, Herberg S, Periyasamy-Thandavan S, Bhatia K, Hafez SS, Johnson MH, Hill WD, Ergul A, Fagan SC, et al. Remote ischemic perconditioning is effective alone and in combination with intravenous tissue-type plasminogen activator in murine model of embolic stroke. *Stroke*. 2012;43:2794–2799. doi: 10.1161/STROKEAHA.112.660373
20. Hess DC, Hoda MN, Khan MB. Humoral mediators of remote ischemic conditioning: important role of eNOS/NO/nitrite. *Acta Neurochir Suppl*. 2016;121:45–48. doi: 10.1007/978-3-319-18497-5_8
21. Rassaf T, Totzeck M, Hendgen-Cotta UB, Shiva S, Heusch G, Kelm M. Circulating nitrite contributes to cardioprotection by remote ischemic preconditioning. *Circ Res*. 2014;114:1601–1610. doi: 10.1161/CIRCRESAHA.114.303822
22. Starkopf J, Bugge E, Ytrehus K. Preischemic bradykinin and ischaemic preconditioning in functional recovery of the globally ischaemic rat heart. *Cardiovasc Res*. 1997;33:63–70. doi: 10.1016/s0008-6363(96)00195-2
23. Wu L, Wei M, Zhang B, Zhang B, Chen J, Wang S, Luo L, Liu S, Li S, Ren C, et al. Safety and tolerability of direct ischemic postconditioning following thrombectomy for acute ischemic stroke. *Stroke*. 2023;54:2442–2445. doi: 10.1161/STROKEAHA.123.044060
24. Chen HS, Cui Y, Li XQ, Wang XH, Ma YT, Zhao Y, Han J, Deng CQ, Hong M, Bao Y, et al; RICAMIS Investigators. Effect of remote ischemic conditioning vs usual care on neurologic function in patients with acute moderate ischemic stroke: the RICAMIS randomized clinical trial. *JAMA*. 2022;328:627–636. doi: 10.1001/jama.2022.13123
25. Zeng Q, Huang P, Wang Z, Wei L, Lin K. Remote ischemic conditioning in the treatment of acute cerebral infarction: a case control study. *Heliyon*. 2023;9:e18181. doi: 10.1016/j.heliyon.2023.e18181
26. Blauenfeldt RA, Hjort N, Valentin JB, Homburg AM, Modrau B, Sandal BF, Gude MF, Hougaard KD, Damgaard D, Poulsen M, et al. Remote ischemic conditioning for acute stroke: the RESIST randomized clinical trial. *JAMA*. 2023;330:1236–1246. doi: 10.1001/jama.2023.16893
27. Fury W, Park KW, Wu Z, Kim E, Woo MS, Bai Y, Macdonald LE, Croll SD, Cho S. Sustained increases in immune transcripts and immune cell trafficking during the recovery of experimental brain ischemia. *Stroke*. 2020;51:2514–2525. doi: 10.1161/STROKEAHA.120.029440
28. Grassivaro F, Menon R, Acquaviva M, Ottoboni L, Ruffini F, Bergamaschi A, Muzio L, Farina C, Martino G. Convergence between microglia and peripheral macrophages phenotype during development and neuroinflammation. *J Neurosci*. 2020;40:784–795. doi: 10.1523/JNEUROSCI.1523-19.2019
29. Plemel JR, Stratton JA, Michaels NJ, Rawji KS, Zhang E, Sinha S, Baaklini CS, Dong Y, Ho M, Thorburn K, et al. Microglia response following acute demyelination is heterogeneous and limits infiltrating macrophage dispersion. *Sci Adv*. 2020;6:eaay6324. doi: 10.1126/sciadv.aay6324
30. Zrzavy T, Machado-Santos J, Christine S, Baumgartner C, Weiner HL, Butovsky O, Lassmann H. Dominant role of microglial and macrophage innate immune responses in human ischemic infarcts. *Brain Pathol*. 2018;28:791–805. doi: 10.1111/bpa.12583
31. Jordao MJC, Sankowski R, Brendecke SM, Sagar, Locatelli G, Tai YH, Tay TL, Schramm E, Armbruster S, Hagemeyer N, et al. Single-cell profiling identifies myeloid cell subsets with distinct fates during neuroinflammation. *Science*. 2019;363:7554. doi: 10.1126/science.aat7554
32. Honarpisheh P, Lee J, Banerjee A, Blasco-Conesa MP, Honarpisheh P, d'Aigle J, Mamun AA, Ritzel RM, Chauhan A, Ganesh BP, et al. Potential caveats of putative microglia-specific markers for assessment of age-related cerebrovascular neuroinflammation. *J Neuroinflammation*. 2020;17:366. doi: 10.1186/s12974-020-02019-5
33. Ngai D, Schilperoort M, Tabas I. Efferocytosis-induced lactate enables the proliferation of pro-resolving macrophages to mediate tissue repair. *Nat Metab*. 2023;5:2206–2219. doi: 10.1038/s42255-023-00921-9
34. Gerlach BD, Ampomah PB, Yurdagul A Jr, Liu C, Lauring MC, Wang X, Kasikara C, Kong N, Shi J, Tao W, et al. Efferocytosis induces macrophage proliferation to help resolve tissue injury. *Cell Metab*. 2021;33:2445–2463.e8. doi: 10.1016/j.cmet.2021.10.015
35. Zhao X, Sun G, Zhang J, Strong R, Song W, Gonzales N, Grotta JC, Aronowski J. Hematoma resolution as a target for intracerebral hemorrhage treatment: role for peroxisome proliferator-activated receptor gamma in microglia/macrophages. *Ann Neurol*. 2007;61:352–362. doi: 10.1002/ana.21097
36. Zhao X, Sun G, Ting SM, Song S, Zhang J, Edwards NJ, Aronowski J. Cleaning up after ICH: the role of Nrf2 in modulating microglia function and hematoma clearance. *J Neurochem*. 2014;133:144–152. doi: 10.1111/jnc.12974
37. Woo MS, Yang J, Beltran C, Cho S. Cell surface CD36 protein in monocyte/macrophage contributes to phagocytosis during the resolution phase of ischemic stroke in mice. *J Biol Chem*. 2016;291:23654–23661. doi: 10.1074/jbc.M116.750018
38. Febbraio M, Hajjar DP, Silverstein RL. CD36: a class B scavenger receptor involved in angiogenesis, atherosclerosis, inflammation, and lipid metabolism. *J Clin Invest*. 2001;108:785–791. doi: 10.1172/JCI14006
39. Husemann J, Loike JD, Anankov R, Febbraio M, Silverstein SC. Scavenger receptors in neurobiology and neuropathology: their role on microglia and other cells of the nervous system. *Glia*. 2002;40:195–205. doi: 10.1002/glia.10148
40. Stewart CR, Stuart LM, Wilkinson K, van Gils JM, Deng J, Halle A, Rayner KJ, Boyer L, Zhong R, Frazier WA, et al. CD36 ligands promote sterile inflammation through assembly of a Toll-like receptor 4 and 6 heterodimer. *Nat Immunol*. 2010;11:155–161. doi: 10.1038/ni.1836
41. Hoebe K, Georgel P, Rutschmann S, Du X, Mudd S, Crozat K, Sovath S, Shamel L, Hartung T, Zähringer U, et al. CD36 is a sensor of diacylglycerides. *Nature*. 2005;433:523–527. doi: 10.1038/nature03253
42. Stuart LM, Deng J, Silver JM, Takahashi K, Tseng AA, Hennessy EJ, Ezekowitz RA, Moore KJ. Response to Staphylococcus aureus requires CD36-mediated phagocytosis triggered by the COOH-terminal cytoplasmic domain. *J Cell Biol*. 2005;170:477–485. doi: 10.1083/jcb.200501113
43. Drage MG, Pecora ND, Hise AG, Febbraio M, Silverstein RL, Golenbock DT, Boom WH, Harding CV. TLR2 and its co-receptors determine responses of macrophages and dendritic cells to lipoproteins of Mycobacterium tuberculosis. *Cell Immunol*. 2009;258:29–37. doi: 10.1016/j.cellimm.2009.03.008
44. Cho S, Park EM, Febbraio M, Anrather J, Park L, Racchumi G, Silverstein RL, Iadecola C. The class B scavenger receptor CD36 mediates free radical production and tissue injury in cerebral ischemia. *J Neurosci*. 2005;25:2504–2512. doi: 10.1523/JNEUROSCI.0035-05.2005
45. Clausen BH, Lambertsen KL, Babcock AA, Holm TH, Dagnaes-Hansen F, Finsen B. Interleukin-1beta and tumor necrosis factor-alpha are expressed by different subsets of microglia and macrophages after ischemic stroke in mice. *J Neuroinflammation*. 2008;5:46. doi: 10.1186/1742-2094-5-46
46. Yurdagul A Jr, Subramanian M, Wang X, Crown SB, Ilkayeva OR, Darville L, Kolluru GK, Rymond CC, Gerlach BD, Zheng Z, et al. Macrophage metabolism of apoptotic cell-derived arginine promotes continual efferocytosis and resolution of injury. *Cell Metab*. 2020;31:518–533.e10. doi: 10.1016/j.cmet.2020.01.001
47. Grajchen E, Wouters E, van de Haterd B, Haidar M, Hardonniere K, Dierckx T, Van Broeckhoven J, Erens C, Hendrix S, Kerdine-Romer S, et al. CD36-mediated uptake of myelin debris by macrophages and microglia reduces neuroinflammation. *J Neuroinflammation*. 2020;17:224. doi: 10.1186/s12974-020-01899-x
48. Kim E, Febbraio M, Bao Y, Tolhurst AT, Epstein JM, Cho S. CD36 in the periphery and brain synergizes in stroke injury in hyperlipidemia. *Ann Neurol*. 2012;71:753–764. doi: 10.1002/ana.23569
49. Nihashi T, Inao S, Kajita Y, Kawai T, Sugimoto T, Niwa M, Kabeya R, Hata N, Hayashi S, Yoshida J. Expression and distribution of beta amyloid precursor protein and beta amyloid peptide in reactive astrocytes after transient middle cerebral artery occlusion. *Acta Neurochir (Wien)*. 2001;143:287–295. doi: 10.1007/s007010170109
50. Hayashi T, Noshita N, Sugawara T, Chan PH. Temporal profile of angiogenesis and expression of related genes in the brain after ischemia. *J Cereb Blood Flow Metab*. 2003;23:166–180. doi: 10.1097/01.WCB.0000041283.53351.CB
51. Pilitsis JG, Coplin WM, O'Regan MH, Wellwood JM, Diaz FG, Fairfax MR, Michael DB, Phillis JW. Measurement of free fatty acids in cerebrospinal fluid from patients with hemorrhagic and ischemic stroke. *Brain Res*. 2003;985:198–201. doi: 10.1016/s0006-8993(03)03044-0
52. Shie FS, Neely MD, Maezawa I, Wu H, Olson SJ, Jürgens G, Montine KS, Montine TJ. Oxidized low-density lipoprotein is present in astrocytes surrounding cerebral infarcts and stimulates astrocyte interleukin-6 secretion. *Am J Pathol*. 2004;164:1173–1181. doi: 10.1016/S0002-9440(10)63205-1

53. Balkaya M, Kröber JM, Rex A, Endres M. Assessing post-stroke behavior in mouse models of focal ischemia. *J Cereb Blood Flow Metab*. 2013;33:330–338. doi: 10.1038/jcbfm.2012.185
54. Springer J, Schust S, Peske K, Tschirner A, Rex A, Engel O, Scherbakov N, Meisel A, von Haehling S, Boschmann M, et al. Catabolic signaling and muscle wasting after acute ischemic stroke in mice: indication for a stroke-specific sarcopenia. *Stroke*. 2014;45:3675–3683. doi: 10.1161/STROKEAHA.114.006258
55. Kronenberg G, Balkaya M, Prinz V, Gertz K, Ji S, Kirste I, Heuser I, Kampmann B, Hellmann-Regen J, Gass P, et al. Exofocal dopaminergic degeneration as antidepressant target in mouse model of poststroke depression. *Biol Psychiatry*. 2012;72:273–281. doi: 10.1016/j.biopsych.2012.02.026
56. Tamura A, Kirino T, Sano K, Takagi K, Oka H. Atrophy of the ipsilateral substantia nigra following middle cerebral artery occlusion in the rat. *Brain Res*. 1990;510:154–157. doi: 10.1016/0006-8993(90)90744-v
57. Hirouchi Y, Suzuki E, Mitsuoka C, Jin H, Kitajima S, Kohjimoto Y, Enomoto M, Kugino K. Neuroimaging and histopathological evaluation of delayed neurological damage produced by artificial occlusion of the middle cerebral artery in Cynomolgus monkeys: establishment of a monkey model for delayed cerebral ischemia. *Exp Toxicol Pathol*. 2007;59:9–16. doi: 10.1016/j.etp.2007.02.008
58. Chang SJ, Cherng JH, Wang DH, Yu SP, Liou NH, Hsu ML. Transneuronal degeneration of thalamic nuclei following middle cerebral artery occlusion in rats. *Biomed Res Int*. 2016;2016:3819052. doi: 10.1155/2016/3819052
59. Fujie W, Kirino T, Tomukai N, Iwasawa T, Tamura A. Progressive shrinkage of the thalamus following middle cerebral artery occlusion in rats. *Stroke*. 1990;21:1485–1488. doi: 10.1161/01.str.21.10.1485
60. El Amki M, Clavier T, Perzo N, Bernard R, Guichet PO, Castel H. Hypothalamic, thalamic and hippocampal lesions in the mouse MCAO model: potential involvement of deep cerebral arteries? *J Neurosci Methods*. 2015;254:80–85. doi: 10.1016/j.jneumeth.2015.07.008
61. Garcia-de-la-Asuncion J, Perez-Griera J, Moreno T, Duca A, Garcia-Del-Olmo N, Belda J, Soro M. Limb ischemic conditioning induces oxidative stress followed by a correlated increase of HIF-1alpha in healthy volunteers. *Ann Vasc Surg*. 2020;62:412–419. doi: 10.1016/j.avsg.2019.06.033
62. Zweier JL, Flaherty JT, Weisfeldt ML. Direct measurement of free radical generation following reperfusion of ischemic myocardium. *Proc Natl Acad Sci USA*. 1987;84:1404–1407. doi: 10.1073/pnas.84.5.1404
63. Cai Z, Zhong H, Bosch-Marce M, Fox-Talbot K, Wang L, Wei C, Trush MA, Semenza GL. Complete loss of ischaemic preconditioning-induced cardioprotection in mice with partial deficiency of HIF-1 alpha. *Cardiovasc Res*. 2008;77:463–470. doi: 10.1093/cvr/cvm035
64. Nagy L, Tontonoz P, Alvarez JG, Chen H, Evans RM. Oxidized LDL regulates macrophage gene expression through ligand activation of PPARgamma. *Cell*. 1998;93:229–240. doi: 10.1016/s0092-8674(00)81574-3
65. Tontonoz P, Nagy L, Alvarez JG, Thomazy VA, Evans RM. PPARgamma promotes monocyte/macrophage differentiation and uptake of oxidized LDL. *Cell*. 1998;93:241–252. doi: 10.1016/s0092-8674(00)81575-5
66. Marcovecchio PM, Thomas GD, Mikulski Z, Ehinger E, Mueller KAL, Blatchley A, Wu R, Miller YI, Nguyen AT, Taylor AM, et al. Scavenger receptor CD36 directs nonclassical monocyte patrolling along the endothelium during early atherogenesis. *Arterioscler Thromb Vasc Biol*. 2017;37:2043–2052. doi: 10.1161/ATVBAHA.117.309123
67. Sun S, Yao Y, Huang C, Xu H, Zhao Y, Wang Y, Zhu Y, Miao Y, Feng X, Gao X, et al. CD36 regulates LPS-induced acute lung injury by promoting macrophages M1 polarization. *Cell Immunol*. 2022;372:104475. doi: 10.1016/j.cellimm.2021.104475
68. Huang SC, Everts B, Ivanova Y, O'Sullivan D, Nascimento M, Smith AM, Beatty W, Love-Gregory L, Lam WY, O'Neill CM, et al. Cell-intrinsic lysosomal lipolysis is essential for alternative activation of macrophages. *Nat Immunol*. 2014;15:846–855. doi: 10.1038/ni.2956
69. Kakarla R, Bhangoo G, Pandian J, Shuaib A, Kate MP. Remote ischemic conditioning to reduce perihematoma edema in patients with intracerebral hemorrhage (RICOCHET): a randomized control trial. *J Clin Med*. 2024;13:2696. doi: 10.3390/jcm13092696
70. Morioka S, Maueroder C, Ravichandran KS. Living on the edge: efferocytosis at the interface of homeostasis and pathology. *Immunity*. 2019;50:1149–1162. doi: 10.1016/j.immuni.2019.04.018
71. Poon IK, Lucas CD, Rossi AG, Ravichandran KS. Apoptotic cell clearance: basic biology and therapeutic potential. *Nat Rev Immunol*. 2014;14:166–180. doi: 10.1038/nri3607
72. Kumar D, Pandit R, Yurdagul A Jr. Mechanisms of continual efferocytosis by macrophages and its role in mitigating atherosclerosis. *Immunometabolism (Cobham)*. 2023;5:e00017. doi: 10.1097/IN9.0000000000000017
73. Benali F, Fladt J, Jaroenngarmsamer T, Bala F, Singh N, Ospel JM, Tymianski M, Hill MD, Goyal M, Ganesh A. Association of brain atrophy with functional outcome and recovery trajectories after thrombectomy: post hoc analysis of the ESCAPE-NA1 trial. *Neurology*. 2023;101:e1521–e1530. doi: 10.1212/WNL.0000000000207700
74. Lee K, Lee H, Kim YD, Nam HS, Lee HS, Yoo J, Cho S, Heo JH. Association of substantia nigra degeneration with poor neurological recovery in basal ganglia infarctions. *J Stroke*. 2023;25:169–172. doi: 10.5853/jos.2022.02145
75. Lee H, Lee K, Kim YD, Nam HS, Lee HS, Cho S, Heo JH. Association between substantia nigra degeneration and functional outcome in patients with basal ganglia infarction. *Eur J Neurol*. 2024;31:e16111. doi: 10.1111/ene.16111
76. Cui Y, Chen YN, Nguyen TN, Chen HS. Time from onset to remote ischemic conditioning and clinical outcome after acute moderate ischemic stroke. *Ann Neurol*. 2023;94:561–571. doi: 10.1002/ana.26715
77. Cui Y, Zhang J, Chen HS. Age and efficacy of remote ischemic conditioning in acute ischemic stroke. *CNS Neurosci Ther*. 2023;30:e14451. doi: 10.1111/cns.14451
78. Blauenfeldt RA, Mortensen JK, Hjort N, Valentin JB, Homburg AM, Modrau B, Sandal BF, Gude MF, Berhndtz AB, Johnsen SP, et al. Effect of remote ischemic conditioning in ischemic stroke subtypes: a post hoc subgroup analysis from the RESIST trial. *Stroke*. 2024;55:874–879. doi: 10.1161/strokeaha.123.046144
79. Zhao W, Hausenloy DJ, Hess DC, Yellon DM, Ji X. Remote ischemic conditioning: challenges and opportunities. *Stroke*. 2023;54:2204–2207. doi: 10.1161/STROKEAHA.123.043279
80. Kim ID, Ju H, Minkler J, Madkoor A, Park KW, Cho S. Obesity-induced Ly6C^{High} and Ly6C^{Low} monocyte subset changes abolish post-ischemic limb conditioning benefits in stroke recovery. *J Cereb Blood Flow Metab*. 2024;44:689–701. doi: 10.1177/0271678x231215101
81. Nagendran J, Pulinilkunnil T, Kienesberger PC, Sung MM, Fung D, Febbraio M, Dyck JR. Cardiomyocyte-specific ablation of CD36 improves post-ischemic functional recovery. *J Mol Cell Cardiol*. 2013;63:180–188. doi: 10.1016/j.yjmcc.2013.07.020
82. Matsushita N, Okada H, Yasoshima Y, Takahashi K, Kiuchi K, Kobayashi K. Dynamics of tyrosine hydroxylase promoter activity during midbrain dopaminergic neuron development. *J Neurochem*. 2002;82:295–304. doi: 10.1046/j.1471-4159.2002.00972.x
83. Kim E, Tolhurst AT, Cho S. Deregulation of inflammatory response in the diabetic condition is associated with increased ischemic brain injury. *J Neuroinflammation*. 2014;11:83. doi: 10.1186/1742-2094-11-83
84. Chi J, Crane A, Wu Z, Cohen PA. A tissue clearing method for three-dimensional imaging of adipose tissue. *J Vis Exp*. 2018;(137):e58271. doi: 10.3791/58271
85. Renier N, Adams EL, Kirst C, Wu Z, Azevedo R, Kohl J, Autry AE, Kadiri L, Umadevi Venkataraju K, Zhou Y, et al. Mapping of brain activity by automated volume analysis of immediate early genes. *Cell*. 2016;165:1789–1802. doi: 10.1016/j.cell.2016.05.007
86. Silversmith W, Zlateski A, Bae JA, Tartavull I, Kemnitz N, Wu J, Seung HS. Igneous: distributed dense 3D segmentation meshing, neuron skeletonization, and hierarchical downsampling. *Front Neural Circuits*. 2022;16:977700. doi: 10.3389/fncir.2022.977700
87. Qin L, Jing D, Parauda S, Carmel J, Ratan RR, Lee FS, Cho S. An adaptive role for BDNF Val66Met polymorphism in motor recovery in chronic stroke. *J Neurosci*. 2014;34:2493–2502. doi: 10.1523/JNEUROSCI.4140-13.2014
88. Kim ID, Ju H, Minkler J, Jiang R, Singh A, Sharma R, Febbraio M, Cho S. Endothelial cell CD36 mediates stroke-induced brain injury via BBB dysfunction and monocyte infiltration in normal and obese conditions. *J Cereb Blood Flow Metab*. 2023;271678:x231154602. doi: 10.1177/0271678x231154602